ECOLE
POLYTECHNIQUE
DE BRUXELLES

ULB

UNIVERSITÉ LIBRE DE BRUXELLES

Differential entropies in phase space for quantum photonic systems

Mémoire présenté en vue de l'obtention du diplôme
d'Ingénieur Civil physicien à finalité Physique appliquée

Zacharie Van Herstraeten

Directeur
Professeur Nicolas Cerf

Superviseur
Michael Jabbour

Service
Service QuIC

Année académique
2016 - 2017

Abstract

This report applies the theory of continuous majorization to quantum phase distributions. To this purpose, we restrict our study to nonnegative Wigner distributions. The physicality conditions in phase space formalism are addressed. Wigner entropy is introduced as the differential entropy of nonnegative Wigner distributions. The initial objective of this report is to prove the conjecture of Hertz, Jabbour and Cerf showing that vacuum is the state of least Wigner entropy. That aim is not reached here, but a scheme of demonstration is proposed. The demonstration involves the properties of pure loss channels and decreasing rearrangements. A majorization criterion is derived using Lindblad equation applied to pure loss channels. That criterion ensures that the instantaneous output of a pure loss channel majorizes its input, under some conditions. Finally, numerical simulations are presented to illustrate the validity of the conjecture.

Keywords : Continuous majorization, decreasing rearrangements, phase space representation, nonnegative Wigner distributions, physicality, entropy, pure loss channels, Lindblad equation.

Résumé

Ce rapport applique la théorie de la majorisation continue aux distributions quantiques dans l'espace des phases. Dans ce but, nous restreignons notre étude aux distributions de Wigner non négatives. Nous abordons les conditions de physicalité dans le formalisme de l'espace des phases. Nous introduisons l'entropie de Wigner comme l'entropie différentielle des fonctions de Wigner non négatives. L'objectif initial de ce rapport est de prouver la conjecture de Hertz, Jabbour et Cerf indiquant que le vide est l'état à l'entropie de Wigner la plus faible. Ce but n'est pas atteint ici, mais nous proposons un schéma de démonstration. La démonstration a recours aux propriétés des canaux à perte pure et des réarrangements décroissants. Un critère de majorisation est établi à partir de l'équation de Lindblad appliquée aux canaux à perte pure. Ce critère assure que la sortie instantanée d'un canal à perte pure majorise son entrée, sous certaines conditions. Pour finir, nous présentons des simulations numériques illustrant la validité de la conjecture.

Mots-clés : Majorisation continue, réarrangements décroissants, représentation dans l'espace des phases, distributions de Wigner non négatives, physicalité, entropie, canaux à perte pure, équation de Lindblad.

Remerciements

Je tiens à remercier toutes les personnes qui d'une manière ou d'une autre m'ont apporté du soutien pour réaliser ce travail.

Je remercie Michael Jabbour pour sa disponibilité et la grande aide qu'il m'a apportée.

Je remercie Monsieur Nicolas Cerf pour le temps précieux qu'il a pu me consacrer.

Je remercie les membres du service QuIC pour leur accueil et leur bienveillance.

Contents

Introduction

Information, however abstract it can be, is part of any system which obeys the laws of physics. Information is physical [18]. What then when these laws are the laws of quantum mechanics, rather than classical physics ? The question is the core of quantum information theory. Quantum information theory is a field of study at the border of quantum mechanics and information theory. It has encountered a major growth in the last forty years, and remarkable discoveries keep being exposed. As examples, let us mention quantum teleportation [6], dense coding [24], quantum cryptography [3] and the no-cloning theorem [32]. The most famous application of quantum information theory is probably the quantum computer. Quantum computers exploit quantum parallelism to perform some tasks faster than any classical computer could ever do. Quantum information is bound to have a bright future.

Quantum mechanics brought to light a phenomenon non-existent in classical mechanics : the Heisenberg uncertainty principle. That fundamental principle is a limitation intrinsic to quantum mechanics. This report is part of a process towards improving our understanding of that limitation. In information theory, entropy is a very appropriate quantity to characterize uncertainty. It can be used to define an entropic uncertainty principle. In this report, we investigate a recent conjecture which is a very natural extension to the entropic uncertainty principle [13].

That conjecture involves the phase space representation of quantum mechanics. A central part of this report is thus devoted to the Wigner quasi-probability distribution. We assign a particular interest to the conditions that it must satisfy in order to ensure its physicality. Also, we look for nonnegative Wigner distributions, as the conjecture only applies to them.

Majorization is a mathematical tool which is subtly designed to compare the uncertainty of distributions; it has already proved to be a powerful theory applicable to quantum physics. We expect majorization will cast new perspectives on the conjecture.

Demonstrating the conjecture hasn't been achieved here. However, we present interesting results, such as a majorization criterion, which constitutes an equivalent condition for the conjecture to be satisfied. In chapter 1, we introduce the general theory of majorization and apply it to 2D probability distributions. Chapter 2 is dedicated to phase space formalism. We give its formulation, and apply it to the field of quantum optics. In chapter 3, we introduce Lindblad equation to describe irreversible quantum processes. This enables us to define pure loss channels, which are physical objects of particular interest as regards disorder. We explain the conjecture and develop how we propose to prove it in chapter 4. We present analytic derivations leading to a majorization criterion. This is our main contribution. Finally, we conclude this report with numerical simulations in chapter 5. We illustrate the validity of the conjecture and make some further observations.

Part I

Background

Chapter 1

Theory of majorization

1.1 Introduction and motivation

In this first chapter, we introduce a mathematical theory known as majorization. The main objective of majorization is to provide a tool to compare the randomness of distributions. Randomness is a rather vague term that requires clarifications. Roughly, randomness is what makes a distribution wider, more spread-out, than a more localized, definite one. Majorization gives a precise formulation of what makes a distribution more random than another.

Majorization takes different forms depending on the type of distributions it is applied to. We talk about discrete majorization when we consider discrete distributions, such as vectors. We talk about continuous majorization when the distributions are continuous functions. Discrete majorization has already found applications to quantum mechanics [25]. Yet, we are not dealing with discrete majorization in this report. One of our aims is to apply the theory of continuous majorization to quantum phase space. This has not been investigated yet.

In section 1.2, we introduce discrete majorization. Discrete majorization is indeed easier to deal with than continuous majorization. The intention is to present the main properties of the discrete case, since they remain in general valid for the continuous case. In section 1.3, we give the generalization of discrete majorization to the continuous case. This requires the introduction of some new notions. Finally, we particularize the results of continuous majorization to 2D distributions in section 1.4.

The main reference that we use is [23]. We also refer to [30] for continuous majorization.

1.2 Discrete majorization

1.2.1 Definition

Definition 1.1. *Vector* $\mathbf{x} = (x_1, ..., x_n)$ *majorizes vector* $\mathbf{y} = (y_1, ..., y_n)$*, written* $\mathbf{x} \succ \mathbf{y}$*, if and only if*

$$\begin{cases} \sum_{i=1}^{k} x_i^{\downarrow} \geq \sum_{i=1}^{k} y_i^{\downarrow} & \text{for } k = 1, ..., n-1 \quad (1.2.1a) \\ \sum_{i=1}^{n} x_i^{\downarrow} = \sum_{i=1}^{n} y_i^{\downarrow} & (1.2.1b) \end{cases}$$

with $\mathbf{x}, \mathbf{y} \in \mathbb{R}^n$*, and* $x_i^{\downarrow}$ *is the* i^{th} *highest component of* $\mathbf{x}$*.*

If vectors $\mathbf{x}$ and $\mathbf{y}$ describe probability distributions, we have:

$$x_i \geq 0, \qquad y_i \geq 0, \qquad \sum_{i=1}^{n} x_i = \sum_{i=1}^{n} y_i = 1 \tag{1.2.2}$$

so that equation 1.2.1b is always satisfied.

1.2.2 Disorder

It may not yet appear clearly that $\mathbf{x} \succ \mathbf{y}$ translates to "$\mathbf{x}$ is more ordered than $\mathbf{y}$". A condition equivalent to 1.2.1 can be derived, and exhibits more openly the difference of randomness [12]. This condition involves the concept of bistochastic matrices, that we define hereafter. In this subsection we consider that $\mathbf{x}$ and $\mathbf{y}$ are probability distributions so that equation 1.2.2 is satisfied.

Definition 1.2. *The square matrix* B *is bistochastic if its elements are nonnegative and if its rows and columns each sum up to 1.*

$$B = (b_{ij}) \ \textit{bistochastic} \quad \Leftrightarrow \quad \begin{cases} b_{ij} \geq 0 & \forall i, j \\ \sum_j b_{ij} = 1 & \forall i \\ \sum_i b_{ij} = 1 & \forall j \end{cases} \tag{1.2.3}$$

Thanks to bistochastic matrices, majorization condition 1.2.1 can be written alternatively [23].

Property 1.1. $\mathbf{x}$ *majorizes* $\mathbf{y}$ *if and only if there exists a bistochastic matrix* B *such that* $\mathbf{y} = B\mathbf{x}$*.*

$$\mathbf{x} \succ \mathbf{y} \quad \Leftrightarrow \quad \mathbf{y} = B\mathbf{x} \tag{1.2.4}$$

where B *is a bistochastic matrix, and* $\mathbf{x}$ *and* $\mathbf{y}$ *are probability distributions.*

The key to understand that the effect of a bistochastic matrix is comparable to an increase of disorder resides in permutations. Permutations are operations that switch two or more components of a vector. A bistochastic matrix can be expressed as a combination

of permutations weighted by probabilities [12]. If B is a bistochastic matrix, then there exists a probability distribution $\{p_i\}$ such that

$$B = \sum_i p_i \Pi_i \tag{1.2.5}$$

where Π_i are permutation matrices. Therefore, $\mathbf{x}$ majorizes $\mathbf{y}$ means that $\mathbf{y}$ is the average between several mixing of $\mathbf{x}$. This pictures well the fact that $\mathbf{y}$ is more disordered than $\mathbf{x}$.

Let us now consider two extreme cases of distributions : the completely determined distribution $\mathbf{a} = (1, 0, ..., 0)$ and the uniformly random distribution $\mathbf{b} = \left(\frac{1}{n}, ..., \frac{1}{n}\right)$. Obviously, $\mathbf{a} \succ \mathbf{b}$. Moreover,

$$(1, 0, ..., 0) \succ \mathbf{x} \succ \left(\frac{1}{n}, ..., \frac{1}{n}\right) \tag{1.2.6}$$

for all probability distribution $\mathbf{x}$. Indeed, for every vector $\mathbf{x}$, there exist bistochastic matrices A and B such that $\mathbf{x} = A\mathbf{a}$ and $\mathbf{b} = B\mathbf{x}$ [23].

1.2.3 Convexity

What makes majorization a powerful tool is the strong property that it implies. If a majorization relation exists between two vectors, then the following property involving all convex functions holds [23].

Property 1.2. *If $\phi : \mathbb{R} \to \mathbb{R}$ is a convex function:*

$$\mathbf{x} \succ \mathbf{y} \quad \Rightarrow \quad \sum_{i=1}^{n} \phi(x_i) \geq \sum_{i=1}^{n} \phi(y_i) \tag{1.2.7}$$

where $\mathbf{x} = (x_1, ..., x_n), \mathbf{y} = (y_1, ..., y_n) \in \mathbb{R}^n$.

If ϕ is concave, inequality is reversed. Property 1.2 can be extended to a wider class of functions. We introduce the concept of Schur-convexity hereafter. It is closely linked with majorization.

Definition 1.3. *Function $\phi : \mathbb{R}^n \to \mathbb{R}$ is Schur-convex if and only if:*

$$\mathbf{x} \succ \mathbf{y} \quad \Rightarrow \quad \phi(\mathbf{x}) \geq \phi(\mathbf{y}) \tag{1.2.8}$$

where $\mathbf{x}, \mathbf{y} \in \mathbb{R}^n$.

Conversely, function ψ is Schur-concave if its opposite $-\psi$ is Schur-convex. In this case we have $\mathbf{x} \succ \mathbf{y} \Rightarrow \psi(\mathbf{x}) \leq \psi(\mathbf{y})$. A function ϕ that is Schur-convex has to be symmetric, i.e. $\phi(\mathbf{x})$ is invariant under permutation of components of $\mathbf{x}$. Also, all convex functions that are symmetric are Schur-convex, but a Schur-convex function needn't to be convex [28].

1.2.4 Further considerations

Majorization is reflexive:

$$\mathbf{x} \succ \mathbf{x} \qquad \forall \mathbf{x}. \tag{1.2.9}$$

It is transitive:

$$\begin{cases} \mathbf{x} \succ \mathbf{y} \\ \mathbf{y} \succ \mathbf{z} \end{cases} \quad \Rightarrow \quad \mathbf{x} \succ \mathbf{z}. \tag{1.2.10}$$

However, it is not anti-symmetric:

$$\begin{cases} \mathbf{x} \succ \mathbf{y} \\ \mathbf{y} \succ \mathbf{x} \end{cases} \quad \not\Rightarrow \quad \mathbf{x} = \mathbf{y}. \tag{1.2.11}$$

For these reasons, majorization is a pre-order. Moreover, it can happen that both $\mathbf{x} \not\succ \mathbf{y}$ and $\mathbf{x} \not\prec \mathbf{y}$ hold. In this case, $\mathbf{x}$ and $\mathbf{y}$ are said incomparable.

1.3 Continuous majorization

In this section we generalize the previous results to continuous distributions.

1.3.1 Decreasing rearrangement

In the discrete case, we use the notation $\mathbf{x}^{\downarrow}$ to signify that we rearranged vector $\mathbf{x}$. Rearranging a continuous distribution is slightly more subtle, and requires some definitions that we introduce in this subsection. In what follows, we consider a function $f : \mathbb{R}^n \to \mathbb{R}^+$ which is nonnegative and integrable. Decreasing rearrangements are only defined for functions satisfying these conditions.

Subsets of a n-dimensional space can be represented by the topological notion of Borel sets. A Borel set is associated to a n-dimensional volume through a Lebesgue measure. We will use the notation $\nu(A)$ to designate the volume of the Borel set A. We note the open ball of radius r centered at the origin as $B(0, r)$. We define the spherically decreasing rearrangement of a Borel set as follows [30]:

Definition 1.4. *Let A be a Borel set with volume $\nu(A)$. Its spherical rearrangement $A^{\downarrow}$ is the open ball of radius r centered at the origin with volume $\nu(A)$:*

$$A^{\downarrow} = B(0, r) \tag{1.3.1}$$

We are going to use this definition to introduce the decreasing rearrangement of a function. To this purpose, we make use of the layer cake representation [30]. A nonnegative integrable function f can be written as:

$$f(\mathbf{x}) = \int_0^{f(\mathbf{x})} \mathrm{d}t = \int_0^{+\infty} \mathbf{1}_{[0, f(\mathbf{x})]}(t) \mathrm{d}t \tag{1.3.2}$$

where we have used the indicator function $\mathbf{1}_{[0,f(\mathbf{x})]}(t)$. This function of t is equal to unity when $0 \leq t < f(\mathbf{x})$ and is zero otherwise.

We now define the Borel set A_t as the set of points that have a value higher than t:

$$A_t = \{\mathbf{x} : f(\mathbf{x}) > t\}, \tag{1.3.3}$$

so that we can write the indicator function as:

$$\mathbf{1}_{[0,f(\mathbf{x})]}(t) = \{\mathbf{x} \in A_t\} \tag{1.3.4}$$

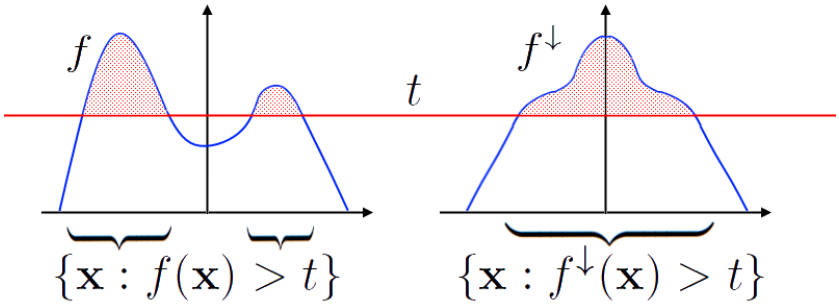

Figure 1.1 – Schematic representation of the rearrangement of a continuous function. $f^{\downarrow}$ is the decreasing rearrangement of f. $f^{\downarrow}$ is a decreasing function symmetric with respect to the origin, such that it has the same level function as f. On the figure, the portion of the axis that has a value higher than t has the same length for f and $f^{\downarrow}$. Formally, this reads : $\nu\left(\{\mathbf{x} : f(\mathbf{x}) > t\}\right) = \nu\left(\{\mathbf{x} : f^{\downarrow}(\mathbf{x}) > t\}\right)$.

where $\{\mathbf{x} \in A_t\}$ is equal to unity when $\mathbf{x}$ belongs to the set A_t and is zero otherwise. The layer cake representation of function f then resumes to:

$$f(\mathbf{x}) = \int_0^{+\infty} \{\mathbf{x} \in A_t\} \mathrm{d}t. \tag{1.3.5}$$

Definition 1.5. *The decreasing rearrangement $f^{\downarrow}$ of the nonnegative integrable function f is*

$$f^{\downarrow}(\mathbf{x}) = \int_0^{+\infty} \{\mathbf{x} \in A_t^{\downarrow}\} \mathrm{d}t \tag{1.3.6}$$

1.3.2 Level function

Definition 1.6. *The level function of the nonnegative integrable function f is*

$$m_f(t) = \nu(\{\mathbf{x} : f(\mathbf{x}) > t\}) \tag{1.3.7}$$

where $t \geq 0$.

The level function $m_f(t)$ gives the n-dimmensional volume of points $\mathbf{x}$ that have a value $f(\mathbf{x})$ higher than t [20].

Property 1.3. *The level function m_f is invarriant under rearrangement:*

$$m_f(t) = m_{f^{\downarrow}}(t) \tag{1.3.8}$$

From its construction, the decreasing rearrangement of a function preserves its level function. Building the decreasing rearrangement of a function consists in computing a decreasing function that has the same level function. Figure 1.1 illustrates the notions of decreasing rearrangements and level functions in a one-dimensional case.

1.3.3 Definition

Definition 1.7. *Function f majorizes function g, written $f \succ g$, if and only if*

$$\begin{cases} \int\limits_{B(0,r)} f^{\downarrow}(\mathbf{x})\mathrm{d}\mathbf{x} \geq \int\limits_{B(0,r)} g^{\downarrow}(\mathbf{x})\mathrm{d}\mathbf{x} \qquad \forall r \geq 0 & \text{(1.3.9a)} \\ \int\limits_{\mathbb{R}^n} f^{\downarrow}(\mathbf{x})\mathrm{d}\mathbf{x} = \int\limits_{\mathbb{R}^n} g^{\downarrow}(\mathbf{x})\mathrm{d}\mathbf{x} & \text{(1.3.9b)} \end{cases}$$

This definition is a generalization of definition 1.2.1. It holds for continuous and multidimensional distributions. If f and g are defined on $\mathbb{R}^2$, we are in the case of 2D distributions and ν is a measure of area.

1.3.4 Convexity

Property 1.4. *If $\phi : \mathbb{R} \to \mathbb{R}$ is a continuous convex function such that $\phi(0) = 0$:*

$$f \succ g \quad \Rightarrow \quad \int\limits_{\mathbb{R}^n} \phi\left(f(\mathbf{x})\right)\mathrm{d}\mathbf{x} \geq \int\limits_{\mathbb{R}^n} \phi\left(g(\mathbf{x})\right)\mathrm{d}\mathbf{x}. \tag{1.3.10}$$

The inequality is reversed for concave functions. This property is the analogue of property 1.2. We now define Schur-convexity in the context of continuous distributions.

Definition 1.8. *Function $\Phi : \mathcal{A} \to \mathbb{R}$ is Schur-convex if and only if*

$$f \succ g \quad \Rightarrow \quad \Phi(f) \geq \Phi(g), \tag{1.3.11}$$

where $\mathcal{A}$ is the set of integrable nonnegative functions $\mathbb{R}^n \to \mathbb{R}^+$ and $f, g \in \mathcal{A}$.

Conversely, function Ψ is Schur-concave if its opposite $-\Psi$ is Schur-convex, and we have $f \succ g \Rightarrow \Psi(f) \leq \Psi(g)$.

1.4 Application to 2D distributions

Previous section is quite abstract and very mathematical. We now particularize the general results of continuous majorization to 2D probability distributions. A probability distributions is a normalized nonnegative distribution. In what follows, we will consider that these properties are respected:

$$\int\limits_{-\infty}^{+\infty}\int\limits_{-\infty}^{+\infty} F(x,y)\mathrm{d}x\mathrm{d}y = 1, \qquad F(x,y) \geq 0 \quad \forall (x,y) \tag{1.4.1}$$

1.4.1 Symmetric decreasing rearrangement

The symmetric decreasing rearrangement of a 2D distribution is the decreasing circular symmetric distribution that has the same level function as the original distribution [9]. A symmetric decreasing rearrangement is completely defined by its decreasing radial function.

The level function of a 2D distribution $F(x, y)$ follows from definition 1.3.7:

$$m_F(t) = \text{Area}(\{(x, y) : F(x, y) > t\}) \tag{1.4.2}$$

$m_F(t)$ is the area of the distribution that has a value higher than t. We want to create the symmetric decreasing distribution that has the same level function. Taking advantage of the symmetry of the rearrangement, we can compute its level function from its radial function. Let $F^{\downarrow}(r)$ be the radial function of the decreasing rearrangement. Since it is decreasing, we know that all the points higher than a certain value t are inside a disc of radius $\left(F^{\downarrow}\right)^{-1}(t)$. $\left(F^{\downarrow}\right)^{-1}$ is the inverse of function $F^{\downarrow}$. We can thus write:

$$m_{F^{\downarrow}}(t) = \pi \left[\left(F^{\downarrow}\right)^{-1}(t)\right]^2 \tag{1.4.3}$$

where t can be evaluated between 0 and $\sup F$. Moreover, the level function is invariant under rearrangement : $m_{F^{\downarrow}} = m_F$. Using inversion rule for compositions of functions, we can rewrite previous equation as:

$$F^{\downarrow}(r) = m_F^{-1}\left(\pi r^2\right). \tag{1.4.4}$$

Equation 1.4.4 links the radial function $F^{\downarrow}$ to the level function m_F of the original distribution F. It tells us the recipe to build symmetric decreasing rearrangements of nonnegative 2D distribution. Computing the level function is an inevitable step. Indeed, majorization compares the level functions of distributions.

1.4.2 Cumulative sum

Note that for normalized distributions, equation 1.3.9b is always satisfied. Majorization condition resumes to 1.3.9a and reads as follows for 2D distributions:

$$F \succ G \quad \Leftrightarrow \quad 2\pi \int_0^r F^{\downarrow}(R) R \mathrm{d}R \geq 2\pi \int_0^r G^{\downarrow}(R) R \mathrm{d}R \quad \forall r \geq 0. \tag{1.4.5}$$

We now introduce the cumulative sum of a function as the integral of its decreasing rearrangement:

$$S_F(r) = 2\pi \int_0^r F^{\downarrow}(R) R \mathrm{d}R. \tag{1.4.6}$$

Cumulative sums allow us to write condition of majorization in the following form:

$$F \succ G \quad \Leftrightarrow \quad S_F(r) \geq S_G(r) \quad \forall r \geq 0 \tag{1.4.7}$$

In practice we will use the latter condition to check majorization.

Chapter 2

Continuous-variable quantum information

2.1 Introduction and motivation

In quantum mechanics, we distinguish continuous variable systems and discrete variables systems. A discrete variable system is a quantum system which is described by observables that have discrete spectra. A qubit is such a system, and is associated to observables such as spin or polarization. On the contrary, a continuous variable system is discribed by observables with continuous spectra. In this report, we will consider continuous variable systems that are described by the continuous observables position and momentum.

The aim of this chapter is to introduce the phase space representation of quantum mechanics. To this purpose we define some basics notions of quantum mechanics. We start this chapter with a succinct overview of the density operator formalism in section 2.2. We focus on the aspect that we will use in this report, such as physicality and disorder. Section 2.3 is the central element of this chapter. We introduce there the phase space formulation of quantum mechanics strictly speaking. We compare this representation to the density matrix under several aspects. Finally we apply the phase formalism to quantum optics is section 2.4. Quantum optics is the physical background of this report. We define several states that have particular properties.

The main references are [2] and [26] for section 2.2. In section 2.3, we have mostly used [19], [10] and [33]. For section 2.4, we refer to [19], [2] and [31].

For the sake of clarity, we choose to use units such that $\hbar = 1$. We will use this convention throughout this report.

2.2 Density matrix

In this section, we introduce the basics notions of the density matrix formalism. This is the most widespread representation of quantum mechanics.

2.2.1 Pure and mixed states

A pure state is described by a ket $|\psi\rangle$, which belongs to a Hilbert space $\mathcal{H}$. It has a wave function in the position basis $\psi(q)$, and a wave function in the momentum basis

$\phi(p)$. These two functions are linked through a Fourier transformation:

$$\psi(q) = \frac{1}{\sqrt{2\pi}} \int_{-\infty}^{\infty} \phi(p) e^{iqp} \mathrm{d}p = \langle q|\psi\rangle \tag{2.2.1a}$$

$$\phi(p) = \frac{1}{\sqrt{2\pi}} \int_{-\infty}^{\infty} \psi(q) e^{-iqp} \mathrm{d}q = \langle p|\psi\rangle = \tilde{\psi}(p) \tag{2.2.1b}$$

A mixed state is a state that is not completely determined and exhibits statistical properties. It has probabilities to be in different pure states. The formalism of the density matrix allows us to deal with both pure states and mixed states on a similar way. A mixed state that has the probabilities $\{p_i\}$ to be in the states $\{|\psi_i\rangle\}$ is represented by the density operator $\hat{\rho}$:

$$\hat{\rho} = \sum_i p_i \left|\psi_i\right\rangle \left\langle\psi_i\right| = \sum_i p_i \hat{P}_i \tag{2.2.2}$$

where the operator $\hat{P}_i = \left|\psi_i\right\rangle \left\langle\psi_i\right|$ is the projector of the state $|\psi_i\rangle$. Pure states are a particular case of mixed states where there is only one state with probability 1. The density operator then comes down to a single projector.

2.2.2 Physicality

Any operator $\hat{\rho}$ is an acceptable density matrix if it is normalized (2.2.3a), hermitian (2.2.3b) and nonnegative (2.2.3c). A nonnegative operator is an operator whose eigenvalues are all nonnegative. We will refer to this property as positivity.

$$\begin{cases} \mathrm{Tr}\hat{\rho} = 1 & \text{(2.2.3a)} \\ \hat{\rho}^\dagger = \hat{\rho} & \text{(2.2.3b)} \\ \left\langle u\right| \hat{\rho} \left|u\right\rangle \geq 0 \qquad \forall \left|u\right\rangle & \text{(2.2.3c)} \end{cases}$$

In terms of eigenvalues $\{\lambda_i\}$, these conditions mean respectively that $\sum_i \lambda_i = 1$, $\lambda_i \in \mathbb{R}$ and $\lambda_i \geq 0$. These conditions are obvious if we remember that the eigenvalues of a density operator are probabilities. Note that the eigenvalues may differ from the probabilities $\{p_i\}$ used in equation 2.2.2. Indeed, if the operator $\hat{\rho}$ is initially defined as a mixture of non orthogonal states, the diagonalization of $\hat{\rho}$ will reveal new probabilities. The probabilities $\{\lambda_i\}$ are associated to orthogonal states.

2.2.3 Purity and entropy

Measures of disorder have a particular interest in this report, as they allow to quantify uncertainty. In this context, we introduce the purity of a density operator $\hat{\rho}$ as the quantity γ.

$$\gamma = \mathrm{Tr}\left[\hat{\rho}^2\right] = \sum_i \lambda_i^2 \tag{2.2.4}$$

The purity of pure states is equal to unity, and is strictly lower than 1 for mixed states. In practice, the purity scales from 0 to 1 and is a measure of the degree of mixture of

the state. Another quantity used to measure the uncertainty of a state is von Neumann entropy:

$$S = -\mathrm{Tr}\left[\hat{\rho}\ln\hat{\rho}\right] = -\sum_i \lambda_i \ln\lambda_i \tag{2.2.5}$$

Von Neumann entropy is equal to zero for pure states and can take arbitrarily large values for mixed states. The higher von Neumann entropy is, the less information we have about the state of $\hat{\rho}$.

2.3 Quantum phase probability distribution

Phase space formulation has proved to be a useful representation of statistical phenomenons in classical mechanics. This formalism describes the state of a system as a probability distribution to be in a certain value of position q and momentum p. However, this representation appears untenable when it comes to quantum mechanics. Quantum mechanics indeed forbids the simultaneous knowledge of position q and momentum p. This observation is known as the uncertainty principle.

We are going to see that it is possible to overcome this apparent complication. A phase space formulation of quantum mechanics holds, and it proposes an alternative to the usual density matrix representation that we presented in previous section. This adaptation has nevertheless fundamental differences with the classical phase space representation, as we could expect from the quantum world.

2.3.1 Weyl transform

The central element of quantum phase space representation is a transformation that maps an operator to a corresponding phase distribution. That transformation is the Weyl transform and is defined hereafter.

Definition 2.1. *The Weyl transform of the operator $\hat{A}$ is the function A:*

$$A(q,p) = \frac{1}{2\pi}\int_{-\infty}^{+\infty} \exp(\mathrm{i}px)\left\langle q-\frac{x}{2}\right|\hat{A}\left|q+\frac{x}{2}\right\rangle \mathrm{d}x \tag{2.3.1}$$

Note that even if this is not apparent in definition 2.1, position and momentum operators play a complementary role in the transformation. Indeed, the Weyl transform of $\hat{A}$ is formally equivalent to:

$$A(q,p) = \frac{1}{2\pi}\int_{-\infty}^{+\infty} \exp(\mathrm{i}qy)\left\langle p+\frac{y}{2}\right|\hat{A}\left|p-\frac{y}{2}\right\rangle \mathrm{d}y \tag{2.3.2}$$

What makes that transformation powerful is a property that we will call the overlap formula [19].

Property 2.1. *The Weyl transform satisfies the overlap formula:*

$$\mathrm{Tr}\left[\hat{\mathrm{A}}_1\hat{\mathrm{A}}_2\right] = 2\pi \int_{-\infty}^{+\infty}\int_{-\infty}^{+\infty} A_1(q,p)A_2(q,p)\mathrm{d}q\mathrm{d}p \tag{2.3.3}$$

where A_1 and A_2 are the Weyl transform of respectively $\hat{A}_1$ and $\hat{A}_2$.

Let us consider a straight implication of that property. It can be seen from 2.3.1 that the Weyl transform of identity operator $\hat{\mathbb{I}}$ is $1/2\pi$. We have thus:

$$\mathrm{Tr}\hat{A} = \int_{-\infty}^{+\infty}\int_{-\infty}^{+\infty} A(q,p)\mathrm{d}q\mathrm{d}p. \tag{2.3.4}$$

2.3.2 Wigner distribution function

Let us now turn to the Weyl transform of density operators describing physical states.

Definition 2.2. *The Wigner quasi-probability distribution $W(q,p)$ of a state described by the density operator $\hat{\rho}$ is the Weyl transform of $\hat{\rho}$.*

$$W(q,p) = \frac{1}{2\pi}\int_{-\infty}^{+\infty} \exp(\mathrm{i}px)\left\langle q-\frac{x}{2}\right|\hat{\rho}\left|q+\frac{x}{2}\right\rangle \mathrm{d}x \tag{2.3.5}$$

Note that for a pure state $|\psi\rangle$ with wave functions $\psi(q)$ and $\phi(p)$, relation 2.3.5 becomes:

$$W(q,p) = \frac{1}{2\pi}\int_{-\infty}^{+\infty} \exp(\mathrm{i}px)\psi\left(q-\frac{x}{2}\right)\psi^*\left(q+\frac{x}{2}\right)\mathrm{d}x \tag{2.3.6a}$$

$$= \frac{1}{2\pi}\int_{-\infty}^{+\infty} \exp(\mathrm{i}qy)\phi\left(p+\frac{y}{2}\right)\phi^*\left(p-\frac{y}{2}\right)\mathrm{d}y \tag{2.3.6b}$$

The WDF[1] W of a mixed state $\hat{\rho}$ having eigenvalues $\{\lambda_i\}$ and eigenstates $\{|\psi_i\rangle\}$ is the weighted sum of the WDF of each eigenstate:

$$W = \sum_i \lambda_i W_i \tag{2.3.7}$$

where W_i is the WDF of the state $|\psi_i\rangle$.

2.3.3 Comparison with classical probability distributions

The WDF behaves like a classical phase distribution under several aspects. First, let us consider the expectation value of operator $\hat{A}$ on state $\hat{\rho}$.

$$\mathrm{Tr}\left[\hat{\rho}\hat{A}\right] = 2\pi \int_{-\infty}^{+\infty}\int_{-\infty}^{+\infty} W(q,p)A(q,p)\mathrm{d}q\mathrm{d}p \tag{2.3.8}$$

1. We refer to Wigner distribution functions through the acronym WDF.

where W is the WDF of $\hat{\rho}$ and A the Weyl transform of $\hat{A}$. This relation is another direct implication of the overlap formula (2.3.3). What is remarkable in this writing is that it is completely similar to what we would have classically if we wanted to evaluate the physical quantity $2\pi A(q,p)$ in the classical phase space density $W(q,p)$.

Moreover, the marginal distributions of the WDF give the probability distributions for q and p : ρ_q and ρ_p respectively. This is a key feature for a joint probability distribution.

$$\int_{-\infty}^{+\infty} W(q,p)\mathrm{d}p = \langle q|\,\hat{\rho}\,|q\rangle = \rho_q(q), \qquad \int_{-\infty}^{+\infty} W(q,p)\mathrm{d}q = \langle p|\,\hat{\rho}\,|p\rangle = \rho_p(p). \tag{2.3.9}$$

These equalities follow from the application of the overlap formula on operators $\hat{\rho}$, and $|q\rangle\langle q|$ or $|p\rangle\langle p|$.

These are some elements that make the WDF look like a probability distribution. However, some important differences tend to make the WDF a very particular object. The most surprising feature is that the WDF can take negative values. We can feel this necessity by looking at the scalar product of two pure states:

$$\mathrm{Tr}\left[\hat{\rho}_\psi\hat{\rho}_\phi\right] = |\,\langle\psi|\phi\rangle\,|^2 = 2\pi \int_{-\infty}^{+\infty}\int_{-\infty}^{+\infty} W_\psi(q,p)W_\phi(q,p)\mathrm{d}q\mathrm{d}p. \tag{2.3.10}$$

For orthogonal states, this equation has to vanish. This is only possible if the WDFs are not positive everywhere [16].

Also, the WDF is bounded. This is a consequence of the Cauchy-Schwartz inequality on equation 2.3.6.

$$-\frac{1}{\pi} \leq W(q,p) \leq \frac{1}{\pi} \tag{2.3.11}$$

That limitation can be interpreted as a consequence of the uncertainty principle, and forbids very localized states as we could have in a classical point of view.

2.3.4 Physicality of a WDF

We are interested in how the different physicality conditions (2.2.3) translate in phase space formalism. The normalization condition 2.2.3a translates very simply to a normalization condition on the WDF:

$$\int_{-\infty}^{+\infty}\int_{-\infty}^{+\infty} W(q,p)\mathrm{d}q\mathrm{d}p = 1. \tag{2.3.12}$$

The hermicity condition 2.2.3b implies that the WDF takes real values. One can see from the definition of the Weyl transform 2.3.1 that $A^*(q,p) = A(q,p)$ for hermitian operators.

$$W(q,p) \in \mathbb{R} \qquad \forall (q,p) \tag{2.3.13}$$

The translations of the first two conditions are fairly simple. However, this is not the case of the last one. There is no criteria in phase space to let us know whether the corresponding density operator is nonnegative. We have to convert the WDF back in $\hat{\rho}$

to check that condition. This is one big drawback of phase space formalism. Expressed in terms of WDF, that condition reads as follows:

$$\int_{-\infty}^{+\infty}\int_{-\infty}^{+\infty} W(q,p)W_u(q,p)\mathrm{d}q\mathrm{d}p \geq 0 \qquad \forall\,|u\rangle \tag{2.3.14}$$

where W_u is the WDF of the state $|u\rangle$.

2.3.5 Purity and entropy

We now present several way to characterize uncertainty in phase space. As opposed to the phase space, we will sometimes refer to the density matrix representation as the state space. We will see in this subsection that uncertainty in phase space and uncertainty in state space are to very different notions.

Purity in phase space translates easily:

$$\gamma = 2\pi \int_{-\infty}^{+\infty}\int_{-\infty}^{+\infty} W^2(q,p)\mathrm{d}q\mathrm{d}p. \tag{2.3.15}$$

However, no direct translation of von Neumann entropy exists in phase space. Nevertheless, we introduce another entropy that we will call Wigner entropy, and write H. This entropy is the application to WDFs of the differential entropy defined in information theory [11]. Note that this definition is only applicable to nonnegative WDFs. This is an important restriction that we will address later in this report.

Definition 2.3. *The Wigner entropy of the nonnegative WDF W is the quantity H:*

$$H = -\int_{-\infty}^{+\infty}\int_{-\infty}^{+\infty} W(q,p)\ln\left(W(q,p)\right)\mathrm{d}q\mathrm{d}p \tag{2.3.16}$$

Von Neumann entropy and Wigner entropy render two very different aspects of uncertainty. On the one hand, von Neumann entropy corresponds to a statistical uncertainty about state $\hat{\rho}$. It means that we are unsure about the state in which our system is. This entropy can be reduced to zero if we know the state of the system with exactitude. On the other hand, Wigner entropy is associated to an uncertainty on the position and momentum of the state. In quantum mechanics, the uncertainty principle teaches us that a perfect knowledge of position and momentum at the same time of a quantum system is forbidden. That uncertainty is inherent to quantum behavior. In phase space, this translates to the fact that the Wigner function cannot be arbitrarily sharp, and thus that its Wigner entropy cannot be arbitrarily low. Our long run objective is precisely to show that Wigner entropy has a minimal boundary, conjectured as $\ln\pi + 1$. We will explain this conjecture in detail in chapter 4.

We take advantage of this subsection to introduce Rényi entropies.

Definition 2.4. *Rényi entropy of order α of the nonnegative WDF W is the quantity H_α:*

$$H_\alpha = \frac{1}{1-\alpha}\ln\left(\int_{-\infty}^{+\infty}\int_{-\infty}^{+\infty}\left(W(q,p)\right)^\alpha\mathrm{d}q\mathrm{d}p\right) \tag{2.3.17}$$

with $\alpha \geq 0$ and $\alpha \neq 1$.

Rényi entropies form a set of Schur-concave functions. Moreover, in the limit of α approaching 1, H_α tends to Wigner entropy [27]. In the limit of α arbitrarily large, H_α tends to $-\ln(\sup|W|)$. Some physical constraints on physical WDFs find a very natural expression in terms of Rényi entropies.

$$H_1 \geq \ln \pi + 1 \tag{2.3.18a}$$

$$H_2 \geq \ln \pi + \ln 2 \tag{2.3.18b}$$

$$H_\infty \geq \ln \pi \tag{2.3.18c}$$

In equation 2.3.18a, one can recognize the conjecture that we are investigating in this report. Equation 2.3.18b is another formulation of purity 2.3.15. Equation 2.3.18c translates the fact that the WDF is bounded as shows equation 2.3.11.

2.3.6 Further definitions

In this subsection we present some other definitions that we will use in this report. First, we introduce the characteristic function $\tilde{W}(u,v)$, which is defined as the Fourier transform of the WDF.

Definition 2.5. *The characteristic function $\tilde{W}(u,v)$ is the Fourier transform of the WDF $W(q,p)$:*

$$\tilde{W}(u,v) = \int_{-\infty}^{+\infty}\int_{-\infty}^{+\infty} W(q,p)\exp(-\mathrm{i}uq - \mathrm{i}vp)\mathrm{d}q\mathrm{d}p = \mathrm{FT}\left[W(q,p)\right] \tag{2.3.19}$$

Conversely, the WDF is the inverse Fourier transform of the characteristic function:

$$W(q,p) = \frac{1}{4\pi^2}\int_{-\infty}^{+\infty}\int_{-\infty}^{+\infty} \tilde{W}(u,v)\exp(iuq + ivp)\mathrm{d}u\mathrm{d}v = \mathrm{FT}^{-1}\left[\tilde{W}(u,v)\right] \tag{2.3.20}$$

In some cases, the convolution of the WDF with a Gaussian can present interesting properties. Hereafter, we introduce a wide class of convolved WDFs, known as s-parameterized distributions [19]. The definition of such distributions is done through their characteristic function.

Definition 2.6. *The characteristic function of a s-parameterized probability distribution is the function $\tilde{W}(u,v;s)$:*

$$\tilde{W}(u,v;s) = \tilde{W}(u,v)\exp\left(\frac{s}{4}(u^2+v^2)\right) \tag{2.3.21}$$

Performing an inverse Fourier transform on the characteristic function $\tilde{W}(u,v;s)$ gives us the s-parameteized distribution $W(q,p;s)$.

Definition 2.7. *The s-parameterized function is the function $W(q,p;s)$:*

$$W(q,p;s) = \frac{1}{4\pi^2}\int_{-\infty}^{+\infty}\int_{-\infty}^{+\infty} \tilde{W}(u,v;s)\exp\left(iuq + ivp\right)\mathrm{d}u\mathrm{d}v \tag{2.3.22}$$

A WDF is a s-parameterized distribution of parameter $s = 0$.

2.4 Application to quantum optics

In this section, we apply phase space formalism to quantum optics. We first introduce bosonic systems, which describe the electromagnetic field. We then consider several single modes states.

2.4.1 Bosonic systems

The electromagnetic field is efficiently described by bosonic systems. In physics, the particle associated to the electromagnetic field is the photon, which is a boson. We say that a mode of the electromagnetic field is a bosonic mode. A bosonic system is composed of several bosonic modes, each of them corresponding to a quantum harmonic oscillator [31]. Hereafter, we introduce the harmonic oscillator. We then expose how it relates with the electromagnetic field and bosonic systems.

The harmonic oscillator

We first present some results of a widely used problem of quantum mechanics. We don't give the derivations of the results, as they can be found in every introductory quantum mechanics book, such as [2]. The aim is to clarify notations and to introduce results that we will use later.

A harmonic oscillator is a physical system whose Hamiltonian has the following form:

$$\hat{H} = \frac{1}{2}\left(\hat{q}^2 + \hat{p}^2\right). \tag{2.4.1}$$

Hereafter, we define the annihilation operator $\hat{a}$, creation operator $\hat{a}^\dagger$ and number operator $\hat{N}$.

$$\hat{a} = \frac{1}{\sqrt{2}}\left(q + ip\right), \qquad \hat{a}^\dagger = \frac{1}{\sqrt{2}}\left(q - ip\right), \qquad \hat{N} = \hat{a}^\dagger\hat{a} \tag{2.4.2}$$

$\hat{H}$ and $\hat{N}$ share the same eigenstates. $\hat{N}$ is a hermitian operator, contrarily to $\hat{a}$ and $\hat{a}^\dagger$. This means that the eigenvalues of $\hat{N}$ are real, whereas they are complex for $\hat{a}$ and $\hat{a}^\dagger$. The spectrum of operator $\hat{N}$ is the set of nonnegative integers $\mathbb{N}$. From the canonical commutation relation of $\hat{q}$ and $\hat{p}$, we have the commutation relation of $\hat{a}$ and $\hat{a}^\dagger$:

$$[\hat{q}, \hat{p}] = i, \qquad \left[\hat{a}, \hat{a}^\dagger\right] = 1. \tag{2.4.3}$$

The electromagnetic field as a bosonic system

What gives the harmonic oscillator a particular importance is that it governs the behavior of the electromagnetic field. Each mode of the electromagnetic field oscillates like an harmonic oscillator. Appendix A is dedicated to that development.

Hereafter, we are going to explicit how the different modes relate to each other. To this purpose, we follow the development of [31]. N modes of the electromagnetic field form a bosonic system of N modes, which belongs to the tensor product of N Hilbert spaces $\mathcal{H}^{\otimes N}$:

$$\mathcal{H}^{\otimes N} = \bigotimes_{k=1}^{N} \mathcal{H}_k \tag{2.4.4}$$

The total electromagnetic field contains an infinity of modes, and belongs therefore to an infinite-dimensional Hilbert space.

Each of the Hilbert spaces $\mathcal{H}_k$ possesses an annihilation operator $\hat{a}_k$ and a creation operator $\hat{a}_k^\dagger$. The commutations rules of these operators can be expressed in a compact form using the vectorial operator $\hat{\mathbf{b}}$:

$$\hat{\mathbf{b}} = \left(\hat{a}_1, \hat{a}_1^\dagger, ..., \hat{a}_N, \hat{a}_N^\dagger\right)^{\mathrm{T}} \tag{2.4.5}$$

where the superscript T expresses the transposition. The commutations rules read as:

$$\left[\hat{b}_i, \hat{b}_j\right] = \Omega_{ij}, \qquad i, j = 1, ..., 2N \tag{2.4.6}$$

where Ω_{ij} is an element of the $2N \times 2N$ matrix $\mathbf{\Omega}$:

$$\mathbf{\Omega} = \bigoplus_{k=1}^{N} \boldsymbol{\omega} = \begin{pmatrix} \boldsymbol{\omega} & & \\ & \ddots & \\ & & \boldsymbol{\omega} \end{pmatrix}, \qquad \boldsymbol{\omega} = \begin{pmatrix} 0 & 1 \\ -1 & 0 \end{pmatrix}. \tag{2.4.7}$$

In short, two operators acting on different Hilbert spaces commute. The annihilation and creation operators of the same Hilbert space obey the commutation relation 2.4.3. Throughout this report, we will only consider single mode states, which belong to a unique Hilbert space $\mathcal{H}$.

2.4.2 Fock states

Fock states are the eigenstates of number operator $\hat{N}$ and hamiltonian $\hat{H}$. They correspond to states having a number of photons and an energy exactly defined. Therefore, these states have a highly quantum behavior.

Definition 2.8. *The n^{th} Fock state $|n\rangle$ is the eigenstate of operator $\hat{N}$ with eigenvalue n.*

$$\hat{N}\,|n\rangle = n\,|n\rangle \tag{2.4.8}$$

with $n \in \mathbb{N}$.

Note here that we use a convention such that there exists a 0^{th} Fock state, which is the Fock state having the eigenvalue 0.

Their wave functions ψ_n^{F} are

$$\psi_n^{\mathrm{F}}(q) = \pi^{-\frac{1}{4}} 2^{-\frac{n}{2}} \left(n!\right)^{-\frac{1}{2}} H_n(q) \exp\left(-\frac{q^2}{2}\right) \tag{2.4.9}$$

where H_n is the n^{th} Hermit polynomial.

Their WDFs can be computed from their wave functions and have the following form:

$$W_n^{\mathrm{F}}(q,p) = \frac{1}{\pi} (-1)^n L_n\left(2q^2 + 2p^2\right) \exp\left(-q^2 - p^2\right) \tag{2.4.10}$$

where L_n is the n^{th} Laguerre polynomial. We see from the $q^2 + p^2$ dependence that all Fock states have a circular symmetric WDF. Consequently, this is also the case for any mixture of Fock states. We will often use the radial function $W_n^{\mathrm{F}}(r)$ to describe them, using the parameter $r = \sqrt{q^2 + p^2}$.

We also note that the maximum of their WDF in absolute value is localized at $(q, p) = (0, 0)$. The value of the WDF at this position is equal to $1/\pi$ for even Fock states, and $-1/\pi$ for odd Fock states. In both cases, this is the extremal value allowed for a WDF. The radial function of the n^{th} Fock state vanishes n times.

Vacuum

Vacuum is the 0^{th} Fock state and has a mean number of photons equal to 0. The WDF of the vacuum is a simple Gaussian:

$$W_0(q,p) = \frac{1}{\pi}\exp\left(-q^2-p^2\right) \tag{2.4.11}$$

The WDF of the vacuum is nonnegative everywhere. In fact, it is proven that the only pure states having nonnegative WDFs are described by Gaussian WDFs [14]. The Wigner entropy of the vacuum is precisely equal to $\ln\pi + 1$. Vacuum has indeed the property to saturate the uncertainty principle. Throughout this report, we will always refer to the vacuum WDF with W_0.

2.4.3 Coherent states

Coherent states are eigenstates of the annihilation operator.

Definition 2.9. *The coherent state $|\alpha\rangle$ is the eigenstate of the annihilation operator $\hat{a}$ with eigenvalue α.*

$$\hat{a}\,|\alpha\rangle = \alpha\,|\alpha\rangle \tag{2.4.12}$$

with $\alpha \in \mathbb{C}$.

Introducing the displacement operator $\hat{D}(\alpha)$, it can be shown that any coherent state is a displaced vacuum [19].

$$\hat{D}(\alpha) = \exp\left(\alpha\hat{a}^\dagger - \alpha^*\hat{a}\right), \qquad |\alpha\rangle = \hat{D}(\alpha)\,|0\rangle \tag{2.4.13}$$

The WDF of a coherent state is:

$$W_\alpha(q,p) = \frac{1}{\pi}\exp\left(-(q-q_\alpha)^2-(p-p_\alpha)^2\right) \tag{2.4.14}$$

where $\alpha = (q_\alpha + ip_\alpha)/\sqrt{2}$.

Coherent states are often said to be the most classical quantum states. Indeed, they correspond to a minimum uncertainty state localized around (q_α, p_α). These are the quantum states that approach the most classical delta distributions.

2.4.4 Passive states

While Fock states and coherent states are pure states, passive states are mixed states. A passive state is a decreasing mixture of Fock states. This means that in the Fock basis, they are diagonal with decreasing eigenvalues.

Definition 2.10. *A passive state $\hat{\rho}^{\text{p}}$ is a decreasing mixture of Fock states.*

$$\hat{\rho}^{\text{p}} = \sum_n c_n\,|n\rangle\langle n|, \qquad c_n \geq c_{n+1} \quad \forall n \geq 0 \tag{2.4.15}$$

where c_n are decreasing nonnegative coefficients.

A widely used example of passive states are thermal states. They correspond to the particular case where the coefficients c_n follow an exponentially decreasing law, in accordance with Boltzmann distribution of energies.

Extremal passive states

Extremal passive states are a subset of passive states. In the Fock basis, the eignevalues of extremal passive states are all equal.

Definition 2.11. *The n^{th} extremal passive state $\hat{\rho}_n^{\text{e}}$ is the equal mixture of the first n Fock states.*

$$\hat{\rho}_n^{\text{e}} = \frac{1}{n+1} \sum_{k=0}^{n} |k\rangle \langle k| \tag{2.4.16}$$

The interest of extremal passive states is that they form a basis for the set of passive states. Indeed, it can easily be seen that any passive state may be expressed as a mixture of extremal passive states.

Property 2.2. *Any passive state can be expressed as a mixture of extremal passive states.*

$$\hat{\rho}^{\text{p}} = \sum_n c_n \hat{\rho}_n^{\text{e}} \tag{2.4.17}$$

where $c_n \geq 0$.

Moreover, extremal passive states have nonnegative WDFs. The latter property implies that every passive state has a nonnegative WDF. This consequence is particularly interesting in the frame of this report, as we limit our study to nonnegative distributions. We will highlight this property later in this report.

Chapter 3

The pure loss channel as an open quantum system

3.1 Introduction and motivation

In this chaper, we introduce a physical object that we will use in our further developments. A pure loss channel is a medium that can only absorb photons. For example, optical fibers and beam splitters can be modeled as PLCs [1]. PLCs play a particular role in our report, as we believe that they decrease the disorder of WDFs. To this purpose, we are going to investigate how the action of PLCs affects WDFs. We will use an important result of quantum mechanics known as Lindblad's theorem. This theorem formulates irreversible quantum processes in the density matrix representation. We are going to translate this to the phase space formalism.

In section 3.2, we describe how irreversibility emerges from open systems. We then introduce the PLC as a particular open quantum system. Section 3.3 is dedicated to Lindblad equation. We introduce the equation in order to apply it to the PLC. Finally, we develop in section 3.4 the action of PLCs in the pase space formalism.

In section 3.2, we mainly use [8] and [31]. For section 3.3, we refer to [7], [17], [1] and [26]. The derivations of section 3.4 come from [19]. We explain them in detail in appendix B.

3.2 Open quantum systems

In this section, we present open systems from a quantum mechanical point of view. We explain why they obey irreversible dynamics. We then give a qualitative definition of the PLC, and highlight an important property of PLCs.

3.2.1 Quantum irreversibility

Reversible dynamics studies the evolution of systems under reversible transformations. In quantum mechanics, these transformations are unitary operations. Let us consider two different observations:

— Elementary interactions obey reversible dynamics.

— Some processes are irreversible.

1. We refer to pure loss channels through the acronym PLC.

How can irreversibility emerge from reversible operations ? It is possible to conciliate this apparent paradox using a description that we present hereafter.

First, we introduce the notions of closed and open systems. A closed system is a system that doesn't interact with its environment. It can be considered independently of its environment. On the contrary, an open system is a system which interacts with its environment: their evolutions are linked.

We consider a system of interest $\hat{\rho}^{\mathrm{S}}$ coupled with an environment $\hat{\rho}^{\mathrm{E}}$. The global system is $\hat{\rho}^{\mathrm{SE}}$. The system of interest is an open system, as it interacts with the environment. The global system is a closed system and evolves according to reversible dynamics.

In this report, the quantum states of interest we consider are photons of one electromagnetic mode. The environment consists in all the other modes of the electromagnetic field.

We use the subscript t to denote the temporal evolution of the state. Let $\hat{\rho}_0^{\mathrm{SE}}$ be initially described by a tensor product of $\hat{\rho}_0^{\mathrm{S}}$ and $\hat{\rho}_0^{\mathrm{E}}$:

$$\hat{\rho}_0^{\mathrm{SE}} = \hat{\rho}_0^{\mathrm{S}} \otimes \hat{\rho}_0^{\mathrm{E}}. \tag{3.2.1}$$

The global system undergoes a unitary evolution. Let $\hat{U}_t$ be the unitary operator describing the evolution of $\hat{\rho}^{\mathrm{SE}}$ until time t. The state of $\hat{\rho}^{\mathrm{S}}$ corresponds to a partial trace over the environment on state $\hat{\rho}^{\mathrm{SE}}$:

$$\hat{\rho}_t^{\mathrm{SE}} = \hat{U}_t \hat{\rho}_0^{\mathrm{SE}} \hat{U}_t^\dagger, \qquad \hat{\rho}_t^{\mathrm{S}} = \mathrm{Tr}_{\mathrm{E}} \left[\hat{\rho}_t^{\mathrm{SE}} \right] \tag{3.2.2}$$

If we restrict our field of view to the system of interest, we may feel that its evolution is not reversible. Indeed, evolution of $\hat{\rho}^{\mathrm{S}}$ is not governed by unitary operator, but by a partial trace over the environment. Generally, open systems do not follow reversible dynamics. As it appears from our description, this does not contradict the fact that the global system undergoes a unitary evolution. We will see later that an irreversible process can be described by a mapping P_t, which has to satisfy several conditions.

3.2.2 The pure loss channel

We now use the representation that we introduce above to present the PLC. Note that in this subsection, we give a qualitative definition of the PLC. A more rigorous description will be given after introducing the appropriate theory.

Roughly, a pure loss channel is a channel that mixes an input state with vacuum. This mixing is represented by a unitary operation U that acts on the joint system composed of the input $\hat{\rho}$ and the vacuum $|0\rangle\langle 0|$. We write the action of a PLC as $\mathcal{E}$:

$$\mathcal{E}(\hat{\rho}) = \mathrm{Tr}_{\mathrm{E}} \left[U \left(\hat{\rho} \otimes |0\rangle\langle 0|_{\mathrm{E}} \right) U^\dagger \right]. \tag{3.2.3}$$

Figure 3.1 illustrates this formula.

As we know, vacuum is the state of least energy. This explains the denomination "pure loss" of PLCs. Indeed, a state passing in a PLC can only see its energy decrease. This consideration allows us to introduce an important property of PLCs:

Property 3.1. *The vacuum is the fixed point of the PLC.*

$$\mathcal{E}^n(\hat{\rho}) \underset{n \to +\infty}{\longrightarrow} |0\rangle\langle 0| \tag{3.2.4}$$

where $\mathcal{E}^n$ is the successive application of n times the PLC.

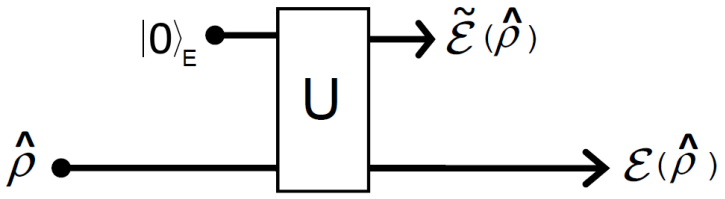

Figure 3.1 – Schematic representation of a PLC. $|0\rangle_E$ is a pure state of the environment, which is chosen to vacuum. $\hat{\rho}$ is the input of the channel, and $\mathcal{E}(\hat{\rho})$ is the output of the channel. $\tilde{\mathcal{E}}(\hat{\rho})$ is the complementary output for the environment. U is a unitary operation. This figure comes from [31].

That property is the reason why we have interest in PLCs. It is conjectured that vacuum is the state of least entropy. We expect to find in the operation performed by a PLC keys to a proof that vacuum is the most ordered state.

3.3 Lindblad master equation

In this section, we address an important result of quantum mechanics. Lindblad master equation formulates irreversible quantum processes in the density matrix representation. We don't give a complete derivation of the equation, as this goes beyond the scope of this report. Rather, we present the main hypothesis assumed, and interpret the final form of the equation.

3.3.1 Markov hypothesis

A major assumption that we lay is that the irreversible process we characterize is Markovian. This means that the evolution of the system only depends on its present state : we don't need to know its past to determine its future. The evolution of the system can then be determined through a mapping P_t [1]:

$$\hat{\rho}_t = P_t(\hat{\rho}_0) \tag{3.3.1}$$

3.3.2 Physicality

The mapping P_t has to verify some conditions in order to ensure the physicality of the system at any time. Obviously, P_t has to be trace-preserving and positivity-preserving. That is to say that a state $\hat{\rho}_0$ which is initially normalized and non-negative must be mapped on another normalized and non-negative state. These two conditions are however not sufficient. The mapping P_t has to satisfy a condition stronger than positivity, known as complete positivity [26]. This condition becomes important when we consider the evolution of entangled states. As an example, if we consider the evolution of a bipartite entangled state, the evolution of one part through a positive mapping can lead to a non-physical state for the bipartite system.

3.3.3 The equation

Bearing these assumptions in mind, we present the result known as Lindblad equation [7]. This result is the most general form of irreversible processes that satisfies the previous requirements. As usual, we use units such that $\hbar = 1$.

$$\frac{\mathrm{d}\hat{\rho}}{\mathrm{d}t} = \mathcal{L}(\hat{\rho}) = i\left[\hat{\rho}, \hat{H}\right] + \sum_i \Gamma_i \left(\hat{L}_i \hat{\rho} \hat{L}_i^\dagger - \frac{1}{2}\hat{L}_i^\dagger \hat{L}_i \hat{\rho} - \frac{1}{2}\hat{\rho}\hat{L}_i^\dagger \hat{L}_i\right) \tag{3.3.2}$$

where $\hat{H}$ is the Hamiltonian of the system, $\hat{L}_i$ arbitrary operators, and Γ_i nonnegative factors. $\mathcal{L}$ is the Linbladian of the system.

We now interpret that equation and give its physical meaning. The term $i\left[\hat{\rho}, \hat{H}\right]$ contains the usual, unitary evolution of the system. Operators $\hat{L}_i$ describe the coupling of the system to its environment. They represent quantum jumps that make $\hat{\rho}$ jump to $\hat{L}_i \hat{\rho} \hat{L}_i^\dagger$ at the rate Γ_i [19]. Irreversibility happens each time a quantum jump occurs.

It can be shown that the time evolution of a WDF evolving under a harmonic Hamiltonian is identical to the classical case : the WDF moves in elliptical paths in phase space [10]. Therefore, we will only consider the part of the time evolution linked to the irreversible process. In what follows, we simply omit the term $i\left[\hat{\rho}, \hat{H}\right]$ in equation 3.3.2.

3.4 Phase distributions in a pure loss channel

In this section, we establish how a state propagating through a PLC sees its WDF affected.

3.4.1 Evolution equation

First, we derive the evolution equation of the WDF in a PLC. The development is rather long, and we choose only to present the key results here. The complete derivation is however done in appendix B. Should any precision be needed, the reader is strongly encouraged to read it.

Absorption is described by the annihilation operator $\hat{a}$. The irreversible part of Lindblad equation 3.3.2 applied to a PLC writes as follows:

$$\frac{\mathrm{d}\hat{\rho}}{\mathrm{d}t} = \Gamma\left(\hat{a}\hat{\rho}\hat{a}^\dagger - \frac{1}{2}\hat{a}^\dagger\hat{a}\hat{\rho} - \frac{1}{2}\hat{\rho}\hat{a}^\dagger\hat{a}\right) \tag{3.4.1}$$

where Γ is the rate of absorption.

This equation describes the evolution of the density matrix. We want to translate it into an evolution equation on the WDF. In order to do so, we need to know the effect of the operators $\hat{a}$ and $\hat{a}^\dagger$ on the WDF. First, we consider the operators $\hat{q}$ and $\hat{p}$. They have the following correspondence rules [19]:

$$\begin{aligned}
\hat{q}\hat{\rho} &\leftrightarrow \left(q + \frac{i}{2}\frac{\partial}{\partial p}\right) W, & \hat{\rho}\hat{q} &\leftrightarrow \left(q - \frac{i}{2}\frac{\partial}{\partial p}\right) W, \\
\hat{p}\hat{\rho} &\leftrightarrow \left(p - \frac{i}{2}\frac{\partial}{\partial q}\right) W, & \hat{\rho}\hat{p} &\leftrightarrow \left(p + \frac{i}{2}\frac{\partial}{\partial q}\right) W.
\end{aligned} \tag{3.4.2}$$

Using the definition of $\hat{a}$ and $\hat{a}^\dagger$ in terms of $\hat{q}$ and $\hat{p}$, these correspondence rules enable us to find the evolution equation of the WDF:

$$\frac{\partial W}{\partial t} = \Gamma \left(W + \frac{q}{2}\frac{\partial W}{\partial q} + \frac{p}{2}\frac{\partial W}{\partial p} + \frac{1}{4}\frac{\partial^2 W}{\partial q^2} + \frac{1}{4}\frac{\partial^2 W}{\partial p^2} \right). \tag{3.4.3}$$

This equation governs the evolution of the WDF. One can check that the vacuum WDF cancels this expression, as we could expect. Vacuum is indeed stationary in a PLC. That equation can be solved analytically in Fourier space. It is done in appendix B. The solution for the characteristic function reads as follows:

$$\tilde{W}(u, v, t) = \tilde{W}\left(u\sqrt{\eta}, v\sqrt{\eta}, 0\right) \exp\left(-(1-\eta)\frac{u^2+v^2}{4} \right) \tag{3.4.4}$$

where $\eta = \exp(-\Gamma t)$ and $\tilde{W}(u, v, t)$ is the characteristic function at time t. In this equation, we have introduced the parameter η that contains the temporal dependence. In practice, a PLC is associated to a certain value of η, which is the parameter of the PLC and scales from 0 to 1. We will refer to the WDF at $t = 0$ as the input of the PLC $W^{(\text{in})}$ and the WDF at time $t = -\ln\eta/\Gamma$ as the output $W^{(\text{out})}$. In this picture, the temporal dependence disappears.

From equation 3.4.4, we see that the characteristic function undergoes a rescaling and a multiplication by a Gaussian. In real space, the WDF undergoes a rescaling and a convolution. We now introduce the norm preserving rescaling operator R_s:

$$R_s\left[A(x, y)\right] = \frac{1}{s^2} A\left(\frac{x}{s}, \frac{y}{s}\right). \tag{3.4.5}$$

This operator enables us to describe the operation performed by a PLC in an elegant way:

$$\boxed{W^{(\text{out})} = R_{\sqrt{\eta}}\left[W^{(\text{in})}\right] * R_{\sqrt{1-\eta}}\left[W_0\right]}. \tag{3.4.6}$$

The output of a PLC is the convolution between the rescaled input and the rescaled vacuum. In the extreme case where $\eta = 1$, $W^{(\text{in})}$ is convoluted with a delta and $W^{(\text{out})} = W^{(\text{in})}$. Conversely, if $\eta = 0$, $W^{(\text{out})} = W_0$.

3.4.2 Disorder

We now consider the transformation performed by the PLC in terms of disorder. A rescaling and a convolution are two very different mechanisms, and have opposed effects as regards disorder.

On the one hand, rescaling is an operation that reduces the support of $W^{(\text{in})}$. It makes it more localized around the origin while preserving its initial shape. This operation lowers the disorder of $W^{(\text{in})}$. On the other hand, a convolution blurs $W^{(\text{in})}$ and modifies its shape. It increases the support of $W^{(\text{in})}$ by making it more diffuse. That operation heightens the disorder of $W^{(\text{in})}$.

In this report, we use the PLC as a tool that inevitably brings WDF closer to the vacuum. It is conjectured that vacuum is the state of least disorder. Therefore, we expect that the operation performed by the PLC decreases the disorder. The disorder increase from the convolution and the disorder decrease from the rescaling should result in a net decrease of disorder.

This condition is deeply linked to the physicality of WDFs. Indeed, we can easily imagine distributions that would undergo an increase of disorder after the action of a PLC. As a simple example, we consider a delta distribution. The increase of disorder it gains from the convolution is not compensated by the rescaling. In this report, we state the hypothesis that all the distributions that gain disorder in a PLC are non-physical.

Part II

Results

Chapter 4

Derivation of a majorization criterion

4.1 Introduction and motivation

In this report, we try to give elements of proof to a recent conjecture proposed in [13]. This chapter is the first one were we present new elements. We suggest here a scheme of demonstration to prove the conjecture. We then expose some analytic derivations towards this aim.

In section 4.2, we give the context of the conjecture. We present a plan of demonstration in section 4.3. This demonstration uses the properties of decreasing rearrangements and pure loss channels. In section 4.4 we give a proof that decreasing rearrangements evolving in PLCs stay decreasing rearrangements. We then derive the equation of evolution of decreasing rearrangements in PLCs in section 4.5. This leads us to a majorization criterion that we explicit in section 4.6. This is the main contribution we give in this report. Finally, we try to give elements that could lead to a complete proof in section 4.7.

4.2 Formulations of uncertainty

In this section, we present several expressions of the observation that we can't have a perfect knowledge of both $\hat{q}$ and $\hat{p}$ at the same time. Each expression formulates a lower bound on the uncertainty of these operators. We are trying to get this bound as tight as quantum physics allows us.

4.2.1 Heisenberg principle

Let us consider two observables that don't commute.

$$\left[\hat{A}, \hat{B}\right] = i\hat{C} \tag{4.2.1}$$

where $\hat{A}$, $\hat{B}$ and $\hat{C}$ are hermitian operators. Showing that the following inequality holds for any state $\hat{\rho}$ is a simple derivation [2].

$$\Delta A \cdot \Delta B \geq \frac{1}{2}\left|\langle \hat{C} \rangle\right| \tag{4.2.2}$$

where we have used the notation

$$\langle \hat{X} \rangle = \mathrm{Tr}\left[\hat{\rho}\hat{X}\right], \qquad \Delta X = \sqrt{\left\langle \hat{X} - \langle \hat{X} \rangle \right\rangle}. \tag{4.2.3}$$

Equation 4.2.2 tells us that it is not possible to have at the same time a perfect knowledge of two observables that don't commute. This inequality finds its most famous writing when applied to the observables position $\hat{q}$ and momentum $\hat{p}$. These operators have the canonical commutation relation $[\hat{q}, \hat{p}] = i$. Heisenberg uncertainty principle reads as follows:

$$\Delta q \Delta p \geq \frac{1}{2}. \tag{4.2.4}$$

4.2.2 Entropic uncertainty

A less known yet tighter inequality can be derived in terms of entropy. The derivation is done for pure states in [4]. Extension to mixed states can be found in [5]. The demonstration is based on relations existing between a function and its Fourier transform. The entropic uncertainty principle reads as follows:

$$H\left[\rho_q\right] + H\left[\rho_p\right] \geq \ln \pi + 1 \tag{4.2.5}$$

where ρ_q and ρ_p are the probability densities for position and momentum respectively. For a state $\hat{\rho}$ having eigenvalues $\{\lambda_i\}$ and eigenstates $\{|\psi_i\rangle\}$, they are given by the following formulas:

$$\rho_q(q) = \sum_i \lambda_i |\psi_i(q)|^2, \qquad \rho_p(p) = \sum_i \lambda_i |\phi_i(p)|^2. \tag{4.2.6}$$

$H\left[\rho\right]$ is the entropy of the distribution ρ and is defined as:

$$H\left[\rho\right] = -\int_{-\infty}^{+\infty} \rho(x) \ln\left(\rho(x)\right) \mathrm{d}x. \tag{4.2.7}$$

What is remarkable about equation 4.2.5 is that it formulates uncertainty by means of entropy, which is, in information theory, a much more usable tool than standard deviation. Moreover, it can be shown that Heisenberg uncertainty principle is a consequence of that inequality [5]. Entropic uncertainty principle is stronger than Heisnberg uncertainty principle.

4.2.3 Uncertainty in phase space

In this subsection, we borrow some notions of information theory [11]. A well known equation of information theory links the entropy of a joint distribution to its marginal entropies:

$$H\left[\rho_{xy}\right] = H\left[\rho_x\right] + H\left[\rho_y\right] - I\left[\rho_{xy}\right] \tag{4.2.8}$$

where $\rho_{xy}(x, y)$ is a joint probability distribution, and $\rho_x(x)$ and $\rho_y(y)$ its marginal probability distributions. $I\left[\rho_{xy}\right]$ is the mutual information of the distribution. Without entering into details, we underline an important property of this quantity : the mutual information is always nonnegative.

It appears thus natural to transcribe the entropic uncertainty principle to a lower bound on the entropy of a joint distribution ρ_{qp}, from which inequality 4.2.5 would directly follow. Wigner quasi-probability distribution is a perfect candidate for ρ_{qp}, since we have seen that its marginal distributions are ρ_q and ρ_p.

However, we encounter a major problem in this interpretation : WDFs can take negative values. The entropy of partially negative distributions is not defined, due to the logarithm function. To make this interpretation complete, one should then define a generalized entropy which would fulfill this gap. This report postpones this necessity, and chooses to only consider nonnegative WDFs.

Baring these considerations in mind, we introduce the conjecture proposed in [13].

Conjecture 4.1. *The Wigner entropy H of a physical nonnegative WDF W satisfies the inequality*

$$H[W] \geq \ln \pi + 1 \tag{4.2.9}$$

That conjecture is stronger than the entropic uncertainty principle. In this report, we present some tracks towards a demonstration. We also give numerical evidences that the conjecture is satisfied.

4.3 Plan of demonstration

In this section, we present a plan that we established in order to prove conjecture 4.1. It is build from four steps, which each constitutes a progress towards a proof. Note that in the process of our research, we had to give slight modifications to this plan. We present here the scheme of demonstration as it was when we started our investigations. All the WDFs that we consider are assumed to be nonnegative.

4.3.1 A stronger conjecture

We propose to use theory of majorization to prove conjecture 4.1. To this purpose, we introduce another conjecture:

Conjecture 4.2. *Any physical nonnegative WDF W is majorized by the vacuum*

$$W \prec W_0 \tag{4.3.1}$$

where W_0 is the WDF of the vacuum.

As we have seen, a relation of majorization is a stronger relation than a difference of entropy. Conjecture 4.1 would be a direct consequence of conjecture 4.2. Entropy is indeed a Schur-concave function, and the Wigner entropy of vacuum is precisely equal to $\ln \pi + 1$.

4.3.2 Rearrangements in a PLC

The main idea of the demonstration is to use a PLC as a disorder decreasing tool. We believe that a WDF passing through a PLC sees its disorder decreased. Indeed, we know from property 3.1 that a WDF in a PLC tends to vacuum.

However, the evolution of a WDF in a PLC may be complicated to characterize in its generality, as WDFs can have very various shapes. To get around this difficulty, we suggest to study the decreasing rearrangements of the WDFs. We know indeed that a relation of majorization is preserved under rearrangement. Therefore, we propose to consider the evolution of the rearrangement in a PLC. We hope that the symmetry of decreasing rearrangements will make the task easier.

The first step of our demonstration is to prove that a decreasing rearrangement evolving in a PLC stays a decreasing rearrangement. In what follows, we denote the evolution through a PLC of parameter η by the operator $\mathcal{E}_\eta$.

Step 4.1. *Prove that PLCs preserve decreasing rearrangements.*

$$\mathcal{E}_\eta\left(W^{\downarrow}\right) = \mathcal{E}_\eta\left(W^{\downarrow}\right)^{\downarrow} \tag{4.3.2}$$

We believe this step should be straightforward to prove, since it appears to our intuition that rescalings and convolutions preserve dereasing rearrangements.

The second step of the demonstration is then to prove that the decreasing rearrangement of a physical WDF is still a physical WDF.

Step 4.2. *Prove that rearranging a nonnegative WDF preserves its physicality.*

$$W \textit{ physical} \quad \Rightarrow \quad W^{\downarrow} \textit{ physical} \tag{4.3.3}$$

This will reveal its importance later. It would ensure us that we study the evolution of a physical system. Note that that step is only a speculation, since we have no clue whether it is the case or not. Rearranging is indeed a rather uncommon operation that no known physical operation uses as a mechanism, on the contrary of convolution, rescaling or rotation for example.

4.3.3 Criterion for majorization

The third step of our demonstration is to find a criterion that a WDF should satisfy in order to be majorized by its instantaneous PLC output. The instantaneous PLC output of a WDF is the output of the WDF through an infinitesimal PLC. This instantaneous evolution is precisely described by Lindblad equation.

Step 4.3. *Formulate a criterion that is a sufficient condition to a majorization by the instantaneous PLC output.*

$$\mathrm{crit}\,(W) \quad \Rightarrow \quad \mathcal{E}_{\eta(\mathrm{d}t)}\,(W) \succ W \tag{4.3.4}$$

We hope to find a criterion that would have a form simple enough to be readily applicable to WDFs.

4.3.4 Physicality as a proof

Finally, last step of this demonstration is to prove that any physical nonnegative WDF satisfies the criterion found in step 4.3.

Step 4.4. *Prove that any physical nonnegative WDF satisfies the criterion.*

$$W \textit{ physical} \quad \Rightarrow \quad \text{crit}(W) \tag{4.3.5}$$

The achievement of the four steps would result to a proof of conjecture 4.2. Indeed, step 4.2 would prove that the rearrangement of any physical WDF is physical. This would mean that the evolution of that rearrangement in a PLC would also be physical at all time. It would thus ensure that the criterion is satisfied at all time, from step 4.4.

If the criterion is satisfied at all time, this would mean from step 4.3 that the evolution of the decreasing rearrangement forms a majorization chain:

$$W^{\downarrow}(t=0) \prec W^{\downarrow}(t=t_1) \prec ... \prec W^{\downarrow}(t=+\infty) \tag{4.3.6}$$

Since we know from property 3.1 that vacuum is the fixed point of a PLC, any state tends to vacuum after a long enough time in a PLC. In equation 4.3.6, we have thus $W^{\downarrow}(t=+\infty) = W_0$. Since a function and its rearrangement are identical from the point of view of majorization, we have:

$$W^{\downarrow} \prec W_0 \quad \Leftrightarrow \quad W \prec W_0. \tag{4.3.7}$$

Consequently, this would lead to a proof of conjecture 4.2. Note that step 4.1 isn't necessary for the proof. However, since it would ensure that the WDF stays a rearrangement in its evolution, it would allow us to formulate a criterion that only relates to decreasing rearrangements.

4.4 Rearrangement in a PLC

As we explained in the previous section, we will restrict our study to the evolution of decreasing rearrangements in a PLC. The fact that a rearrangement is circular symmetric enables us to make some useful simplifications. From now on, we will only consider rearranged WDFs. For readability, we will omit the decreasing symbol, and design $W^{\downarrow}$ by W. Decreasing rearrangements have circular symmetry. For this reason, we can describe them with a one argument function.

$$W(q,p) = W_r(r) \tag{4.4.1}$$

where $r = \sqrt{q^2+p^2}$. Formally, we should make the difference between $W(q,p)$ and $W_r(r)$, which are respectively a two arguments function and a one argument function. However, in what follows, we will designate these two functions by W, without distinction. We use the notation $W'(r) = \frac{\partial}{\partial r}W(r)$. Since W is a decreasing rearrangement, the derivative of its radial function is negative. In what follows, we will consider that the following properties are respected:

$$\begin{cases} W'(r) & \leq 0 \qquad \forall r \geq 0 \\ W(r) & \geq 0 \qquad \forall r \geq 0 \end{cases} \tag{4.4.2}$$

In this section, we prove step 4.1. We remember that the action of a PLC $\mathcal{E}_\eta$ can be decomposed in two distinct operations : a rescaling and a convolution. We are going to prove that the output of these two operations is a decreasing rearrangement if its input is so.

The proof that rescaling preserves decreasing rearrangement is straightforward. It is trivial to show that it preserves circular symmetry. Moreover, we can write:

$$\frac{\partial}{\partial r}\left(R_s\left[W\right]\right) = \frac{\partial}{\partial r}\left(\frac{1}{s^2}W\left(\frac{r}{s}\right)\right) = \frac{1}{s^3}W'\left(\frac{r}{s}\right) \tag{4.4.3}$$

which has the same sign as $W'(r)$. The radial function stays decreasing under rescaling.

The proof that the convolution of a decreasing rearrangement with a Gaussian stays a decreasing rearrangement is slightly trickier. For that reason, we choose not to present this demonstration here. In appendix C, we introduce the notion of bell shaped function, which generalizes the idea of decreasing rearrangement. We then prove that the convolution of two 2D bell shaped functions is a 2D bell shaped function.

We don't dwell on this part of the demonstration, as we would like to focus on the application of majorization in phase space.

4.5 Polar evolution equation

In this section, we derive the evolution of decreasing rearrangements in a PLC, taking its symmetry into account. We then compute its explicit expression.

4.5.1 Evolution equation

We now establish the differential equation of evolution of a polar WDF in a PLC. For readability purpose, we introduce the dimensionless variable $\tau = \Gamma t$.

$$\frac{\partial W}{\partial \tau} = \left(1 + \frac{q}{2}\frac{\partial}{\partial q} + \frac{p}{2}\frac{\partial}{\partial p} + \frac{1}{4}\frac{\partial^2}{\partial q^2} + \frac{1}{4}\frac{\partial^2}{\partial p^2}\right)W \tag{4.5.1}$$

The derivation of the following relations is straightforward:

$$\begin{aligned}
&\frac{\partial}{\partial q}W(r) = W'(r)\frac{q}{r} && \frac{\partial^2}{\partial q^2}W(r) = W''(r)\frac{q^2}{r^2} + W'(r)\left(\frac{1}{r} - \frac{q^2}{r^3}\right)\\
&\frac{\partial}{\partial p}W(r) = W'(r)\frac{p}{r} && \frac{\partial^2}{\partial p^2}W(r) = W''(r)\frac{p^2}{r^2} + W'(r)\left(\frac{1}{r} - \frac{p^2}{r^3}\right)
\end{aligned} \tag{4.5.2}$$

Injecting previous relations in the evolution equation gives us the polar evolution equation:

$$\boxed{\frac{\partial W}{\partial \tau} = W + \left(\frac{r}{2} + \frac{1}{4r}\right)W' + \frac{1}{4}W''} \tag{4.5.3}$$

This partial differential equation describes the evolution of $W(r,t)$ in a PLC. Here, we have only assumed that the WDF is circular symmetric. This equation is also valid for non-decreasing radial functions.

Stationary solution

We may interest ourselves to the polar WDFs that are stationnary in a PLC. In order to do so, we study the ordinary differential equation obtained when equaling the left hand side of 4.5.3 to zero. The equation has two independent solutions:

$$y'' + \left(2x + \frac{1}{x}\right) y' + 4y = 0 \quad \Rightarrow \quad \begin{cases} y = C_1 y_1 + C_2 y_2 \\ y_1 = \exp(-x^2) \\ y_2 = \exp(-x^2)\mathrm{Ei}(x^2) \end{cases} \tag{4.5.4}$$

Ei is the exponential integral. Solution y_2 is not physical since it is unbounded in $x = 0$. Solution y_1 corresponds to the WDF of vacuum. As expected, the vacuum is thus the only polar WDF stationary in a PLC.

4.5.2 Explicit expression

Here, we compute the explicit expression of the evolution. We remember that the evolution of a WDF in a PLC is governed by a rescaling and a convolution. A rescaling is a fairly trivial operation. A convolution of two 2D distributions implies the resolution of two integrals. We will see that when the WDF are circular symmetric, the convolution can be reduced to a unique integral. Using the vectorial notation $\mathbf{r} = (q, p)$, we can write:

$$W^{(\mathrm{out})}(\mathbf{r}) = \frac{1}{\pi\,(1-\eta)} \iint\limits_{\mathbf{R}\in\mathbb{R}^2} W^{(\mathrm{in})}(\mathbf{R}) \exp\left(-\frac{\left(\mathbf{r} - \sqrt{\eta}\mathbf{R}\right)^2}{1-\eta}\right) \mathrm{d}\mathbf{R} \tag{4.5.5}$$

The norm of a vector $\mathbf{a} + \mathbf{b}$ is $\sqrt{a^2 + b^2 + 2ab\cos\theta}$ where a, b and θ are respectively the norm of $\mathbf{a}$, the norm of $\mathbf{b}$ and the angle between $\mathbf{a}$ and $\mathbf{b}$. Some rewriting then gives us:

$$W^{(\mathrm{out})}(r) = \frac{1}{\pi\,(1-\eta)} \int_0^{+\infty} \underbrace{\int_0^{2\pi} \exp\left(\frac{2\sqrt{\eta} r R\cos\theta}{1-\eta}\right) \mathrm{d}\theta}_{2\pi I_0\left(\frac{2\sqrt{\eta} r R}{1-\eta}\right)} W^{(\mathrm{in})}(R) \exp\left(-\frac{r^2 + \eta R^2}{1-\eta}\right) R\mathrm{d}R \tag{4.5.6}$$

I_0 is the modified Bessel function of the first kind. Finally, we find the explicit expression of a polar WDF in a PLC:

$$\boxed{W^{(\mathrm{out})}(r) = \frac{2}{1-\eta} \exp\left(-\frac{r^2}{1-\eta}\right) \int_0^{+\infty} W^{(\mathrm{in})}(R) \exp\left(-\frac{\eta R^2}{1-\eta}\right) I_0\left(\frac{2\sqrt{\eta} r R}{1-\eta}\right) R\mathrm{d}R} \tag{4.5.7}$$

This equation will be useful for numerical simulations.

4.6 Majorization criterion

In the plan of our demonstration, we aim to prove that rearranged physical WDFs are majorized by their instantaneous output through a PLC. We are going to see how this conditions reads using the evolution equation. We consider that conditions 4.4.2 are respected.

4.6.1 Cumulative sum

The majorization condition can be expressed in terms of cumulative sums. The output of a PLC $W^{(\text{out})}$ majorizes its input $W^{(\text{in})}$ if:

$$W^{(\text{out})} \succ W^{(\text{in})} \quad \Leftrightarrow \quad S^{(\text{out})}(r) \geq S^{(\text{in})}(r) \quad \forall r \tag{4.6.1}$$

The cumulative sums $S^{(\text{in})}$ and $S^{(\text{out})}$ can be expressed as functions of $W^{(\text{in})}$ and $W^{(\text{out})}$, respectively. Let $W(t)$ describe the evolution of W in the PLC, so that $W^{(\text{in})} = W(t)$ and $W^{(\text{out})} = W(t + \delta t)$. Similarly, we write $S^{(\text{in})} = S(t)$ and $S^{(\text{out})} = S(t + \delta t)$.

Now, we consider an infinitesimal PLC. This means that $W^{(\text{in})}$ and $W^{(\text{out})}$ are separated by an infinitesimal interval of time. We need thus to consider the limit case where δt tends to 0 with positive values. According to this, we rewrite the condition for majorization as:

$$\begin{aligned}
\lim_{\delta t \to 0^+} (W(t + \delta t)) \succ W(t) \quad &\Leftrightarrow \quad \lim_{\delta t \to 0^+} (S(t + \delta t) - S(t)) \geq 0 \\
&\Leftrightarrow \quad \lim_{\delta t \to 0^+} \left(\frac{S(t + \delta t) - S(t)}{\delta t} \, \delta t \right) \geq 0 \\
&\Leftrightarrow \quad \frac{\partial S}{\partial t} \left(\lim_{\delta t \to 0^+} \delta t \right) \geq 0.
\end{aligned}$$

Since δt tends to zero with positive values, the condition for instantaneous majorization resumes to the nonnegativity of the time derivative of the cumulative sum:

$$W^{(\text{out})} \succ W^{(\text{in})} \quad \Leftrightarrow \quad \frac{\partial S}{\partial t} \geq 0 \quad \forall r \quad \Leftrightarrow \quad 2\pi \int_0^r \frac{\partial W}{\partial t}(R) R \mathrm{d}R \quad \forall r$$

where $W^{(\text{out})}$ is the instantaneous PLC output of $W^{(\text{in})}$.

Let us now explicit the time evolution of the cumulative sum S for a decreasing rearrangement in a PLC:

$$\begin{aligned}
\frac{\partial S}{\partial \tau} &= 2\pi \int_0^r \frac{\partial W}{\partial \tau} R \mathrm{d}R \\
&= 2\pi \int_0^r \left[W + \left(\frac{R}{2} + \frac{1}{4R} \right) W' + \frac{1}{4} W'' \right] R \mathrm{d}R \\
&= 2\pi \left[\int_0^r W R \mathrm{d}R + \frac{1}{2} \int_0^r W' R^2 \mathrm{d}R + \frac{1}{4} \int_0^r W' \mathrm{d}R + \frac{1}{4} \int_0^r W'' R \mathrm{d}R \right]
\end{aligned} \tag{4.6.2}$$

Using integration by parts, we can state:

$$\int_0^r W' R^2 \mathrm{d}R = W r^2 - 2 \int_0^r W R \mathrm{d}R, \qquad \int_0^r W'' R \mathrm{d}R = W' r - \int_0^r W' \mathrm{d}R \tag{4.6.3}$$

These expressions simplify surprisingly well, so that 4.6.2 resumes to:

$$\frac{\partial S}{\partial \tau} = 2\pi \left(\frac{r^2}{2} W + \frac{r}{4} W' \right) \tag{4.6.4}$$

And the majorization criterion becomes:

$$\boxed{W' + 2rW \geq 0} \tag{4.6.5}$$

Theorem 4.1. *Let $W(r)$ be the radial function of a decreasing rearrangement. If W satisfies*

$$W'(r) + 2rW(r) \geq 0 \quad \forall r \geq 0, \tag{4.6.6}$$

then the decreasing rearrangement is majorized by its output through an infinitesimal PLC.

Note that in our hypothesis, $W \geq 0$ and $W' \leq 0$. This criterion can be seen has a an upper bound on the derivative of W:

$$|W'| \leq 2rW \tag{4.6.7}$$

It teaches us that a function whose rearrangement decreases too abruptly does not satisfy the criterion. We presume that this type of function are non physical. Moreover, one can easily check that the vacuum cancels the expression of the criterion.

4.6.2 Level function

We have to keep in mind that majorization is first and foremost a condition on the level function. Decreasing rearrangements have a particular interest as they are directly connected to that level function.

$$W(r) = m^{-1}(\pi r^2) \tag{4.6.8}$$

for decreasing rearrangements, where $m(t)$ is the level function of W as defined in chapter 1. We can write the majorization criterion in term of level function:

$$\pi \frac{\partial}{\partial t} m^{-1}(t) + m^{-1}(t) \geq 0 \tag{4.6.9}$$

where t is evaluated at πr^2. Since this equation has to be satisfied for all $r \geq 0$, it also has to be the case for all $t \geq 0$. On can here recognize the logarithmic derivative of function m^{-1}. Indeed, previous equation can be written as:

$$\boxed{\frac{\partial}{\partial t} \left(\ln m^{-1}(t) \right) \geq -\frac{1}{\pi}} \tag{4.6.10}$$

where this inequality has to be satisfied for all $t \geq 0$ to ensure majorization by vacuum. By construction, the level function has a negative derivative. This equation is the translation of 4.6.5 to the level function. It has the advantage to be directly applicable to any WDF, without passing by its decreasing rearrangement. Indeed, we know that the level function is invariant under rearrangement.

4.6.3 Other formulation

Equation 4.6.5 can be written in an elegant way using an artifice of calculation. The product rule for derivatives tells us that the criterion is equivalent to the following condition:

$$\frac{\partial}{\partial r}\left(\exp\left(r^2\right)W(r)\right) \geq 0 \tag{4.6.11}$$

Now, we remember that the WDF of vacuum is precisely a Gaussian of unitary standard deviation. The criterion can equivalently be written:

$$\boxed{\frac{\partial}{\partial r}\left(\frac{W}{W_0}\right) \geq 0} \tag{4.6.12}$$

where W_0 is the WDF of vacuum. This writing is remarkable inasmuch as it explicitly involves vacuum. This reinforces us in the idea that this criterion is indeed an equivalent condition to majorization by vacuum.

4.7 Towards a proof

We have proved step 4.1 and found the criterion of step 4.3. We now have to prove steps 4.2 and 4.4. Unfortunately, this ambition couldn't be achieved in this report. Attempts were made to prove step 4.4, but it has been unsuccessful for the moment. Concerning step 4.2, we have quite bad news, since it appears from our numerical simulations that decreasing rearrangements of physical WDFs are not necessarily physical. We will address this problem in the next chapter.

We may thus think that our demonstration is doomed to fail. We argue that it is not the case, through some adaptations of our initial scheme. To this purpose, we suggest to introduce two new steps that would replace steps 4.2 and 4.4. These are the following:

Step 4.5. *Prove that the decreasing rearrangement of any physical nonnegative WDF satisfies the criterion.*

$$W \text{ physical} \quad \Rightarrow \quad \text{crit}\left(W^{\downarrow}\right) \tag{4.7.1}$$

Step 4.6. *Prove that if a decreasing rearrangement satisfies the criterion, then its evolution in a PLC satisfies the criterion at all time.*

$$\text{crit}\left(W^{\downarrow}(t=0)\right) \quad \Rightarrow \quad \text{crit}\left(W^{\downarrow}(t=t_1)\right) \quad \forall t_1 \geq 0 \tag{4.7.2}$$

where $W^{\downarrow}(t)$ describes the evolution of $W^{\downarrow}$ in a PLC.

The proof of these two steps would give a complete demonstration of conjecture 4.2. Indeed, this would imply that the evolution of the decreasing rearrangements form a majorization chain, as schematized in equation 4.3.6. The difference here is that the majorization chain would contain non physical WDFs. Majorization is a very mathematical condition, and can be applied on physical as well as non-physical WDFs. What we are aiming to prove is a majorization relation between two physical distributions. The starting point and the ending point of the PLC evolution correspond to rearrangement of physical WDFs. Therefore, it is not a problem if the intermediate distributions are not physical.

Chapter 5

Numerical simulations

5.1 Introduciton and motivation

This last chapter gives a numerical overview of the considerations we introduced in chapter 4. The presence of a chapter devoted to numerical simulations in a very theoretical report may surprise. We know indeed that a numerical simulation will never be enough to serve as a proof. In this chapter, we aim to a better understanding of the mechanisms involved in the evolution of Wigner distributions.

In section 5.2 we describe the method we use to generate nonnegative WDFs that are physically acceptable. In section 5.3, we verify numerically that the different conjectures we exposed are satisfied. Section 5.4 addresses the question of the physicality of decreasing rearrangements. Section 5.5 is devoted to the evolution of WDFs in a PLC. Finally, we expose in section 5.6 an observation involving another kind of majorization, known as Fock majorization.

Our simulations were conducted in Matlab. Program files were coded for the purposes of this project, and can be found in appendix D.

As usual, we use the convention to chose units such that $\hbar = 1$, so that we can express q and p without dimensions. When the WDF has circular symmetry, we use the parameter $r = \sqrt{q^2 + p^2}$.

5.2 Random nonnegative WDF

The first step required to verify numerically our conjecture is to generate random physical states. In this report, we restrict our study to states that have a nonnegative WDF, since majorization is only defined for nonnegative distributions. As we learned previously, it is difficult to check the physicality of a WDF. We cannot simply generate normalized 2D distributions, since they will generally correspond to operators that have negative eigenvalues. We need to build nonnegative WDF that are physical. We present three different ways to achieve that.

5.2.1 Passive states

We stated previously that passive states have the property to have circular symmetric nonnegative WDFs. The 10 first passive extremal states are plotted in figure 5.1. We can thus generate a continuum of random passive states. We take a random set of nonnegative

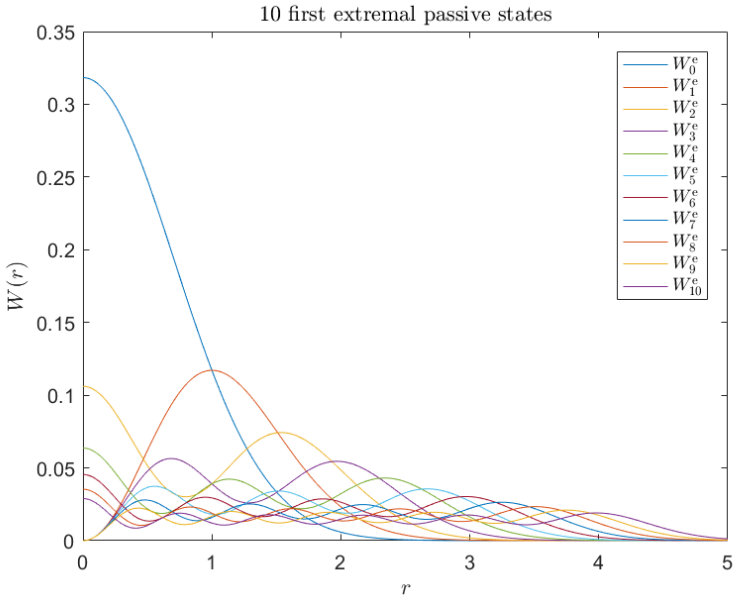

Figure 5.1 – Radial function of the 10 first extremal states. W_n^{e} is the n^{th} extremal passive state.

numbers that sum up to 1. We then create a mixture of extremal passive states with the so-obtained eigenvalues.

5.2.2 Husimi function

In chapter 2, we briefly introduced the s-parameterized probability distribution $W(q,p;s)$. The Husimi function Q is the s-parameterized distribution of parameter $s=-1$ [19].

$$Q(q,p) = W(q,p;-1) \tag{5.2.1}$$

From the definition of s-parameterized distributions, one can see that Husimi function is the convolution of the WDF with vacuum. It has been shown that smoothing a WDF with a Gaussian produces another physically acceptable WDF [22]. Moreover, one can see that Husimi function is necessarily nonnegative:

$$\begin{aligned} Q(q,p) &= \frac{1}{\pi}\int_{-\infty}^{+\infty}\int_{-\infty}^{+\infty} W(q',p')\exp\left(-(q-q')^2-(p-p')^2\right)\mathrm{d}q'\mathrm{d}p' \\ &= \int_{-\infty}^{+\infty}\int_{-\infty}^{+\infty} W(q',p')W_\alpha(q',p')\mathrm{d}q'\mathrm{d}p' \\ &= \frac{1}{2\pi}\mathrm{Tr}\left[\hat{\rho}\left|\alpha\right\rangle\left\langle\alpha\right|\right] = \frac{1}{2\pi}\left\langle\alpha\right|\hat{\rho}\left|\alpha\right\rangle \geq 0 \end{aligned} \tag{5.2.2}$$

where W_α is the WDF of the coherent state $|\alpha\rangle$, $\alpha=(q+ip)/\sqrt{2}$, and we use the overlap formula. We see that the Husimi function is directly proportional to the probability of measuring a coherent state, which must be nonnegative.

We now have another technique to produce random nonnegative WDF that are physically acceptable. We compute the WDF of an arbitrary pure state. To create a random

pure state, we start from its wave function and compute its WDF. Theoretically, any normalized function whose derivative is continuous is acceptable. However, we restrict ourselves to wave functions that are superpositions of the 10 first Fock states in this report. This way, we can ensure that WDFs don't expand too far from the origin. This WDF will in general be partly negative. We then convolve this WDF with the vacuum and get a physical nonnegative WDF.

In comparison with passive states, we have here access to a wider set of random WDFs. Indeed, while passive states had circular symmetric WDF, the WDF that we generate hereby are in general non symmetric.

5.2.3 Pure Loss Channel

The previous result can be slightly improved. For this, we take interest to the evolution of WDF through a PLC of parameter $\eta = 1/2$. The evolution is governed by equation:

$$\begin{aligned} W_{(\text{out})} &= R_{\sqrt{\frac{1}{2}}}\left[W_{(\text{in})}\right] * R_{\sqrt{\frac{1}{2}}}\left[W_0\right] \\ &= R_{\sqrt{\frac{1}{2}}}\left[W_{(\text{in})} * W_0\right] \\ &= R_{\sqrt{\frac{1}{2}}}\left[Q_{(\text{in})}\right] \end{aligned} \tag{5.2.3}$$

where we used that $R_s\left[W_1\right] * R_s\left[W_2\right] = R_s\left[W_1 * W_2\right]$, which is straightforward:

$$\begin{aligned} R_s\left[W_1\right] * R_s\left[W_2\right] &= \frac{1}{s^4} \int_{-\infty}^{+\infty}\int_{-\infty}^{+\infty} W_1\left(\frac{q'}{s}, \frac{p'}{s}\right) W_2\left(\frac{q'-q}{s}, \frac{p'-p}{s}\right) \mathrm{d}q'\mathrm{d}p' \\ &= \frac{1}{s^2} \int_{-\infty}^{+\infty}\int_{-\infty}^{+\infty} W_1\left(q'', p''\right) W_2\left(q'' - \frac{q}{s}, p'' - \frac{p}{s}\right) \mathrm{d}q''\mathrm{d}p'' \\ &= R_s\left[W_1 * W_2\right] \end{aligned} \tag{5.2.4}$$

It appears that the output of such a PLC is the Husimi function of the input, rescaled by a factor $1/\sqrt{2}$. Since this WDF is the result of a physical operation, it must correspond to a physical state.

From now on, we designate the output of the PLC of parameter $\eta = 1/\sqrt{2}$ as W^{plc}, and the Husimi function of the input as Q. What makes this solution more interesting than the mere Husimi function is precisely the rescaling. It means that W^{plc} has a smaller

extent and is more localized than Q. This translate to a difference in their entropies:

$$\begin{aligned}
H[W^{\mathrm{plc}}] &= -\int_{-\infty}^{+\infty}\int_{-\infty}^{+\infty} W^{\mathrm{plc}}(q,p)\ln\left(W^{\mathrm{plc}}(q,p)\right)\mathrm{d}q\mathrm{d}p \\
&= -\int_{-\infty}^{+\infty}\int_{-\infty}^{+\infty} 2Q\left(\sqrt{2}q,\sqrt{2}p\right)\ln\left(2Q\left(\sqrt{2}q,\sqrt{2}p\right)\right)\mathrm{d}q\mathrm{d}p \\
&= -\int_{-\infty}^{+\infty}\int_{-\infty}^{+\infty} Q\left(q',p'\right)\ln\left(2Q\left(q',p'\right)\right)\mathrm{d}q'\mathrm{d}p' \\
&= -\int_{-\infty}^{+\infty}\int_{-\infty}^{+\infty} Q\left(q',p'\right)\ln\left(Q\left(q',p'\right)\right)\mathrm{d}q'\mathrm{d}p' - \ln 2\int_{-\infty}^{+\infty}\int_{-\infty}^{+\infty} Q\left(q',p'\right)\mathrm{d}q'\mathrm{d}p' \\
&= H\left[Q\right] - \ln 2
\end{aligned} \tag{5.2.5}$$

We can even go further and prove that $W^{\mathrm{plc}} \succ Q$. Obviously, their decreasing rearrangement obey the relation : $W^{\mathrm{plc}\downarrow}(r) = 2Q^{\downarrow}\left(\sqrt{2}r\right)$.

$$W^{\mathrm{plc}} \succ Q \quad \Leftrightarrow \quad 2\pi\int_0^r W^{\mathrm{plc}\downarrow}(R)R\mathrm{d}R \geq 2\pi\int_0^r Q^{\downarrow}(R)R\mathrm{d}R \qquad \forall r \tag{5.2.6}$$

$$\Leftrightarrow \quad 2\int_0^r Q^{\downarrow}\left(\sqrt{2}R\right)R\mathrm{d}R \geq \int_0^r Q^{\downarrow}(R)R\mathrm{d}R \qquad \forall r \tag{5.2.7}$$

$$\Leftrightarrow \quad \int_0^{\sqrt{2}r} Q^{\downarrow}\left(R'\right)R'\mathrm{d}R' \geq \int_0^r Q^{\downarrow}(R)R\mathrm{d}R \qquad \forall r \tag{5.2.8}$$

The last equation is obviously satisfied, since $Q^{\downarrow}$ is nonnegative everywhere. What we learn from these considerations is that, between W^{plc} and Q, the WDF which is the more susceptible to break our conjecture is W^{plc}. We will thus prefer the output of a PLC of parameter $\eta = 1/\sqrt{2}$ over the Husimi function in our simulations.

In order to generate the PLC output, we proceed the same way as to create the Husimi function, and we rescale it with a factor $1/\sqrt{2}$.

5.3 Verification of the conjectures

In this section we present the first numerical evidences for the conjectures we introduced previously. Let us first underline that through the entirety of our simulations, whenever we have generated and tested physical states using one of the methods we introduced above, we have found that:

— Wigner entropy is higher than $\ln \pi + 1$.
— The WDF is majorized by the vacuum WDF.
— Majorization criterion is satisfied.

This section is mainly illustrative, and we try to give appropriate examples. In what follows, when we don't specify the parameter η of the PLC, it is assumed $\eta = 1/2$.

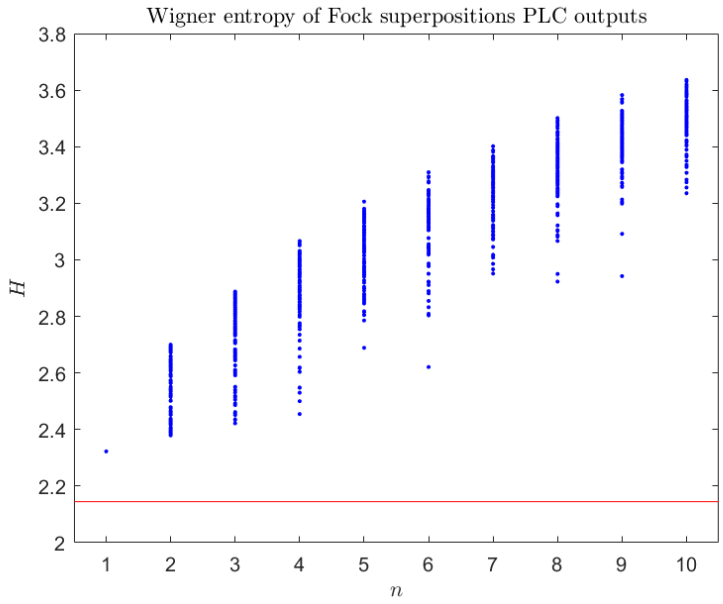

Figure 5.2 – Wigner entropy of the PLC output of superpositions of the first n Fock states. Superpositions are generated using formula 5.3.1. The simulation is repeated 100 times for each value of n. Each dot corresponds to a simulation. Red line is Wigner entropy of vacuum.

5.3.1 Wigner entropy

The first simulation we present is a computation of Wigner entropy for randomly generated states. We create random superpositions of Fock state using the following formula:

$$|\psi_n\rangle = \frac{1}{\sqrt{n+1}} \sum_{k=0}^{n} \exp\left(i\phi_k\right) |k\rangle \tag{5.3.1}$$

where ϕ_k is a random phase uniformly distributed between 0 and 2π. These superpositions have equal amplitude in modulus. The randomness is limited to the phase. This choice has been done in order to enhance the reproductibility of the simulation.

We then compute the Wigner entropy for the PLC output of $|\psi_n\rangle$. Results are shown in figure 5.2 for values of n going from 1 to 10. We see that superpositions of a higher number of Fock states have in average a higher entropy. This is not surprising as higher order Fock states have a larger extent.

Note that even if the initial superpositions have the same amplitudes in modulus, they can result to very different entropies. These differences are only due to the phases of the amplitudes. Note also that when $|\psi\rangle$ is a superposition of $|0\rangle$ and $|1\rangle$ with equal amplitudes in modulus, the entropy of its PLC output is independent of the phase.

We often consider specific WDFs, such as extremal passive states W_n^{e}. Let us introduce another set of physical nonnegative WDF : the Fock states PLC outputs. We refer to the output of the n^{th} Fock state in a PLC of parameter $\eta = 1/2$ as W_n^{plc}:

$$W_n^{\mathrm{plc}} = \mathcal{E}_{\frac{1}{2}}\left(W_n^{\mathrm{F}}\right) \tag{5.3.2}$$

We compare the Wigner entropy of Fock states PLC outputs to the entropy of extremal passive states in figure 5.3. We note that $W_0^{\mathrm{plc}} = W_0^{\mathrm{e}} = W_0$. Our simulations showed that

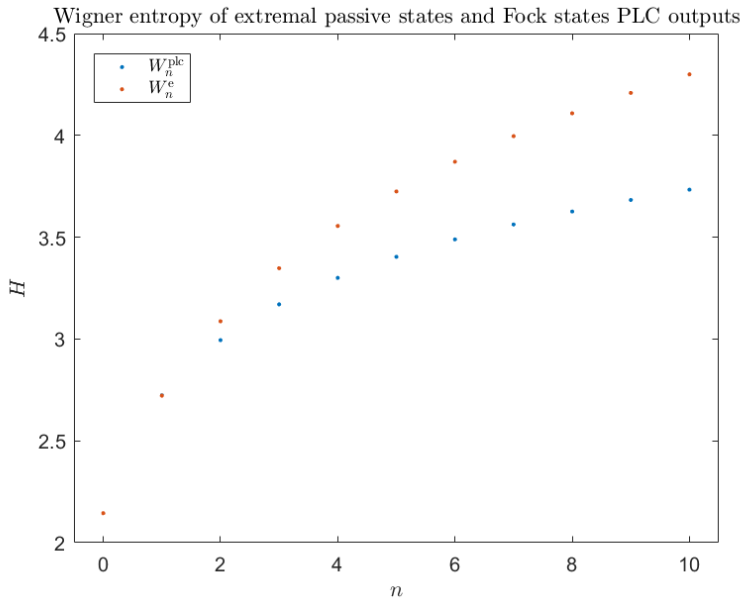

Figure 5.3 – Wigner entropy of Fock states PLC outputs W_n^{plc} and extremal passive states W_n^{e}. It appears that the entropy of Fock states PLC ouputs is lower or equal to the entropy of extremal passive states.

WDFs W_1^{plc} and W_1^{e} coincide.

5.3.2 Majorization by vacuum

To check if a WDF is majorized by vacuum, we use formula 1.4.7. We first build the decreasing rearrangement of the WDF. Then, we compute its cumulative sum, that we compare with the one of vacuum. We cannot be very illustrative in this process. We may only insist on the fact that every physical state that we have tested was majorized by vacuum.

5.3.3 Criterion

Here, we check that Fock states PLC outputs verify the majorization criterion. We consider the states W_n^{plc} for $n = 0$ to 5. To obtain the criterion, we compute decreasing rearrangements and extract their radial functions. We then compute the criterion, which is illustrated in figure 5.4.

5.4 Physicality of a rearrangment

Whether the decreasing rearrangement of a physical WDF is still a physical WDF is an important question. Actually, no obvious argument would let us think that a rearrangement preserves the physicality.

5.4.1 How to check physicality

We are now presenting the method that we use to check the physicality of a WDF. We know that the physicality resumes to 3 conditions. The WDF must be real and normalized,

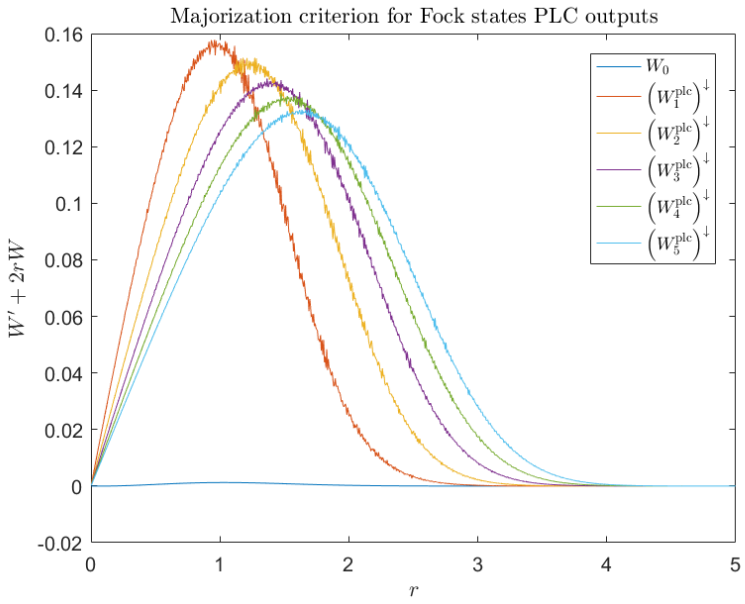

Figure 5.4 – Majorization criterion for the 5 first Fock states PLC outputs W_n^{plc}. As expected, the criterion is nonnegative for all value of r. It appears that for vacuum W_0, the criterion is equal to zero for all r. This result can be found analytically.

and it must correspond to a nonnegative operator $\hat{\rho}$. The latter condition cannot be checked directly on the WDF, and requires that we compute the density operator $\hat{\rho}$.

To check the physicality of a normalized real-valued WDF, we compute $\hat{\rho}$ in the Fock basis, and then diagonalize it. Finally, we check that the eigenvalues are positive. In order to compute $\hat{\rho}$ in the Fock basis, we use the overlap formula:

$$\begin{aligned} \langle i|\,\hat{\rho}\,|j\rangle &= \mathrm{Tr}\left[\hat{\rho}\,|j\rangle\,\langle i|\right] \\ &= 2\pi \int_{-\infty}^{+\infty}\int_{-\infty}^{+\infty} W(q,p)W_{ij}(q,p)\mathrm{d}q\mathrm{q}p \end{aligned} \tag{5.4.1}$$

where W_{ij} is the Weyl transform of operator $|j\rangle\,\langle i|$ and can be obtained using the formula:

$$\begin{aligned} W_{ij}(q,p) &= \frac{1}{2\pi}\int_{-\infty}^{+\infty} \exp(ipx)\left\langle q-\frac{x}{2}\middle|j\right\rangle\left\langle i\middle|q+\frac{x}{2}\right\rangle \mathrm{d}x \\ &= \frac{1}{2\pi}\int_{-\infty}^{+\infty} \exp(ipx)\psi_j\left(q-\frac{x}{2}\right)\psi_i^*\left(q+\frac{x}{2}\right)\mathrm{d}x \end{aligned} \tag{5.4.2}$$

where $\psi_n(x)$ is the wave function of the n^{th} Fock state, vacuum being the 0^{th} Fock state.

Using this method, we should be able to reverse the Weyl transformation and get the operator associated to any WDF. However, we might need to browse a large number of W_{ij}. If we want to compute $\hat{\rho}$ until the n^{th} Fock state, we have to compute $(n+1)(n+2)/2$ WDFs, taken into account that $\hat{\rho}$ is hermitian.

i	λ_i	$\sum_{k=0}^{i} \lambda_k$
0	0.4441	0.4441
1	0.3117	0.7558
2	0.1845	0.9402
3	0.0583	0.9985
4	0.0138	1.0123
5	-0.0204	0.9919
6	0.0054	0.9973
7	0.0010	0.9983
8	0.0027	1.0010
9	-0.0077	0.9933
10	0.0085	1.0018

Table 5.1 – Fock decomposition of the rearrangement of the second extremal passive state $(W_2^{\mathrm{e}})^{\downarrow}$. λ_i is calculated using formula 5.4.4. Simulations bring out that 5^{th} and 9^{th} Fock states have negative components. $(W_2^{\mathrm{e}})^{\downarrow}$ does not correspond to a physical WDF.

Yet, we can simplify this matrix reconstruction if the WDF possesses a circular symmetry. We remember the expression of Fock states WDF:

$$W_n(r) = \frac{1}{\pi}(-1)^n L_n\left(2r^2\right)\exp\left(-r^2\right) \tag{5.4.3}$$

Laguerre polynomials have the interesting property that the set of functions $\{\exp(-x/2) L_n(x)\}$ form a complete orthogonal basis in $L^2(0,\infty)$ [29]. This means that every circular symmetric WDF can be expressed on the basis of Fock WDFs. Because of the orthogonality of the W_{ij}, this also implies that all W_{ij} such that $i \neq j$ have a zero scalar product with circular symmetric WDFs. If we want to test the physicality of a decreasing rearrangement, we can thus limit ourselves to check that all the Fock WDFs have nonnegative components. Fock components λ_n are calculated using the following formula:

$$\lambda_n = 4\pi^2 \int_0^{+\infty} W(r) W_n(r) r \mathrm{d}r \tag{5.4.4}$$

5.4.2 Evidence of non-physicality

Hereafter we present a numerical example of non-physical rearrangement. That example is the decreasing rearrangement of the second extremal state $(W_2^{\mathrm{e}})^{\downarrow}$. Its radial function is pictured in figure 5.5. Table 5.1 shows the numerical decomposition of $(W_2^{\mathrm{e}})^{\downarrow}$ on the 10 first Fock states. We see that some Fock states have negative components in this rearrangement. This is a blatant evidence of the non-physicality of this rearrangement.

Note that the radial function of $(W_2^{\mathrm{e}})^{\downarrow}$ presents abrupt changes in its derivative. This means that its decomposition in Fock states includes quickly variating states, which are Fock states of high order. We highlight that consideration to explain that the sum of the 10 first Fock components is different from unity.

We may thus think that there is no sense in performing a physical operation on a non-physical WDF. It is indeed true that no physical meaning should be given to the evolution

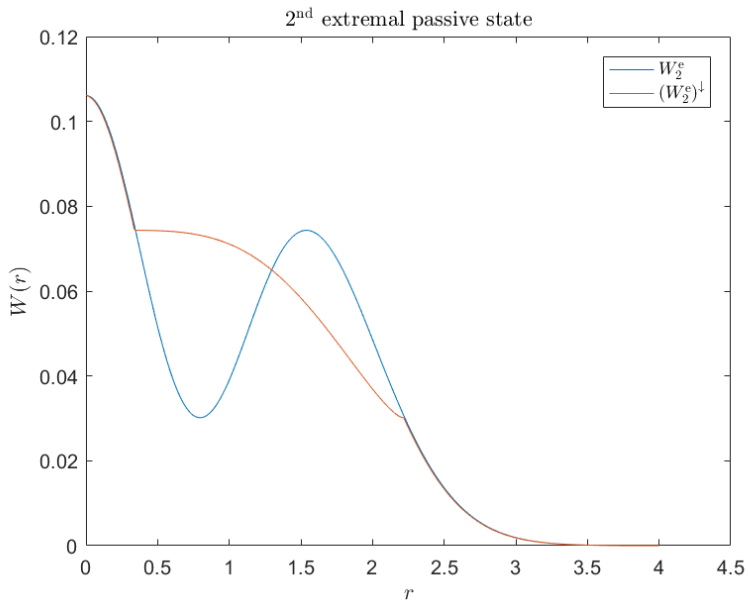

Figure 5.5 – Radial functions of the second extremal passive state W_2^{e} and its decreasing rearrangement $(W_2^{\mathrm{e}})^{\downarrow}$.

of the rearrangement. We have to consider the action of the PLC has a mathematical operation.

5.5 Evolution in a PLC

This section resumes the numerical results of WDFs evolution in a PLC.

5.5.1 Entropy evolution

Naturally, we expect Wigner entropy of a decreasing rearrangement to decrease in a PLC. Our simulations revealed that it is indeed the case. Nevertheless, we are less sure about the fact that this property is also satisfied for non-rearranged WDF. As an example, von Neumann entropy may increase for a state passing through a PLC : a pure state usually exits a PLC as a mixed state. In this subsection, we show numerical illustrations that Wigner entropy seems to always decrease for physical nonnegative WDF passing through a PLC. We have seen that von Neumann and Wigner entropies are very different physical quantities. One applies to state space while to other applies to phase space, and we are not surprised that they behave differently.

To show this phenomenon, we consider the five first Fock states PLC ouputs W_n^{plc}. Figure 5.6 shows the evolution of their respective entropy in time, as well as the entropy of their decreasing rearrangements. From this figure, we can see that Wigner entropy is decreasing at all time. In the limits where t tends to infinity, Wigner entropy $H(t)$ tends to $\ln \pi + 1$. We also note that the entropies of the decreasing rearrangements decrease faster than the non-rearranged WDFs.

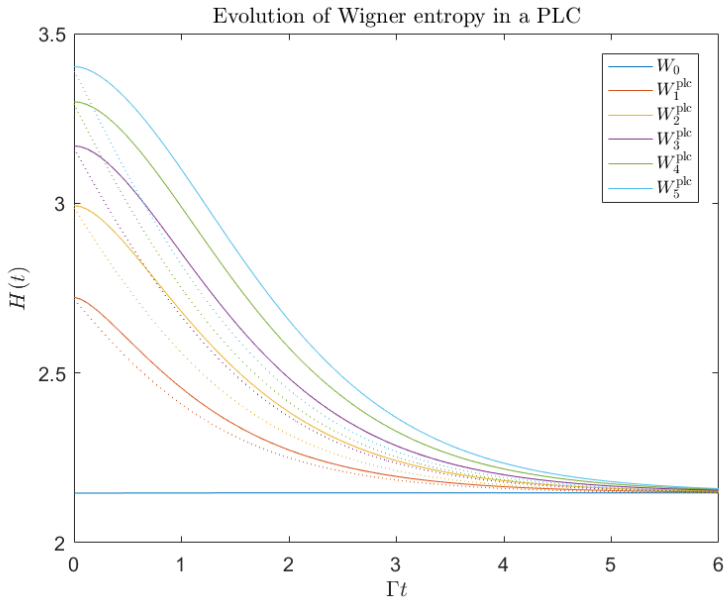

Figure 5.6 – Time evolution of Wigner entropy for Fock states PLC outputs W_n^{plc}. Dotted curves correspond to the entropy evolution of rearranged WDFs $\left(W_n^{\mathrm{plc}}\right)^{\downarrow}$.

5.5.2 Majorization

As for Wigner entropy, we expect the decreasing rearrangement of a physical WDF to be majorized by its PLC ouput, whatever the value of parameter η. This was confirmed by our simulations. We could even go further, and our simulations showed that the relation of majorization is also valid for a non-rearranged physical WDF and its PLC output. Once again, we cannot be very illustrative here.

5.6 Fock majorization

In this last section, we expose another observation we encountered, which involves Fock majorization. It is not directly connected to previous sections, but it presents enough interest for us to explain it hereafter.

Let us first define Fock majorization and clarify its difference with Wigner majorization. On the one hand, Wigner majorization is the majorization that we have been using throughout this report. It uses the theory of continuous majorization in the Wigner distribution. On the other hand, Fock majorization is a majorization relation between two density operators. It uses the theory of discrete majorization, with the difference that eigenvalues are ordered in terms of Fock states rather than in a decreasing order [15]. We distinguish Fock majorization, that we note as $\succ_{\mathrm{F}}$, and Wigner majorization, that we note as $\succ$. Fock majorization reads as follows:

$$\hat{\rho} \succ_{\mathrm{F}} \hat{\sigma} \quad \Leftrightarrow \quad \sum_{i=0}^{k} \lambda_i \geq \sum_{i=0}^{k} \mu_i \quad \forall k \geq 0 \tag{5.6.1}$$

where $\lambda_i = \langle i | \hat{\rho} | i \rangle$ and $\mu_i = \langle i | \hat{\sigma} | i \rangle$ are the eigenvalue of the i^{th} Fock state for $\hat{\rho}$ and $\hat{\sigma}$ respectively. When considering passive states, Fock majorization resumes to regular discrete majorization.

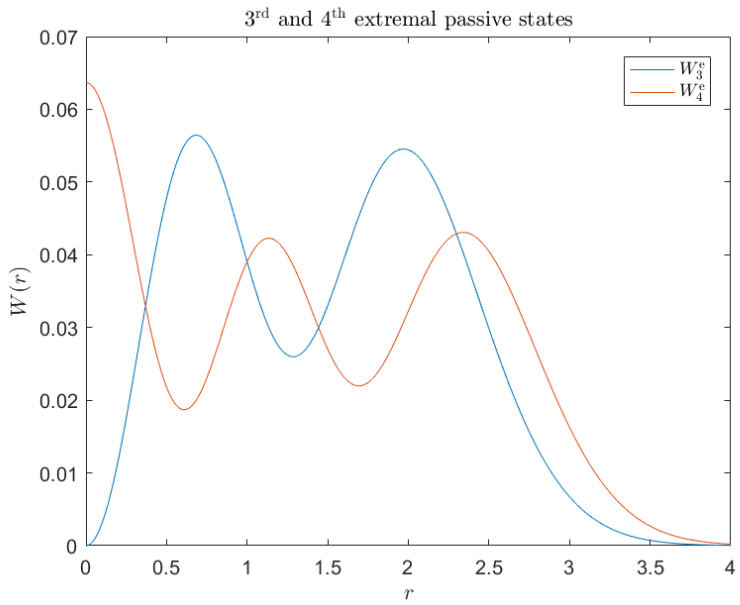

Figure 5.7 – Radial function of 3rd and 4th extremal passive states. It appears that the maximum of W_4^e is higher than the maximum of W_3^e. These two WDF are incomparable.

Our simulations showed that Fock majorization does not imply Wigner majorization. To illustrate this phenomenon, we consider extremal passive states. We designate the n^{th} extremal passive state with its density matrix $\hat{\rho}_n^e$ and its WDF W_n^e.

Using discrete majorization, we have the very straightforward majorization chain:

$$\hat{\rho}_0^e \succ_F \hat{\rho}_1^e \succ_F \ldots \succ_F \hat{\rho}_n^e \succ_F \hat{\rho}_{n+1}^e \tag{5.6.2}$$

We may think that this Fock majorization chain translates naturally to Wigner majorization. It is indeed the case for the first extremal passive states:

$$W_0^e \succ W_1^e \succ W_2^e \succ W_3^e \tag{5.6.3}$$

However, this chain soon breaks off, and we have:

$$W_3^e \not\succ W_4^e, \qquad W_5^e \not\succ W_6^e, \qquad W_7^e \not\succ W_8^e, \qquad W_9^e \not\succ W_{10}^e. \tag{5.6.4}$$

These non-majorization relations can be seen from the fact that the maxima of W_4^e, W_6^e, W_8^e and W_{10}^e are higher than the maxima of respectively W_3^e, W_5^e, W_7^e and W_9^e. Figure 5.7 illustrates the case of W_3^e and W_4^e. WDFs mentionned in equation 5.6.4 form 4 couples of incomparable WDFs. Until the 10^{th} extremal passive state, majorization relations resume to the majorization chain:

$$W_0^e \succ W_1^e \succ W_2^e \succ \begin{matrix} W_3^e \\ W_4^e \end{matrix} \succ \begin{matrix} W_5^e \\ W_6^e \end{matrix} \succ \begin{matrix} W_7^e \\ W_8^e \end{matrix} \succ \begin{matrix} W_9^e \\ W_{10}^e \end{matrix} \tag{5.6.5}$$

Conclusion

In this report, we investigated conjecture 4.1 in the hope of finding tracks towards a demonstration. To this purpose, we made the decision to use the powerful theory of majorization. We were confident that it would be of great use as majorization has already proved to be applicable to quantum mechanics in its discrete form. However, the use of continuous majorization in quantum mechanics is unprecedented. We expected that this fresh approach would give us new results.

In the first part of this report, we tried to give a thorough though concise overview of the different issues involved. The aim was to give to the reader the elements required to understand the conjecture as well as our attempts to demonstrate it. We presented theory of majorization in chapter 1, which focussed on its application to 2D distributions. We introduced notions such as symmetric decreasing rearrangements and level functions, which would be of crucial use in our developments. Chapter 2 was dedicated to the fundamental concepts of quantum mechanics involved in this report. The density matrix was presented. We then defined Wigner distributions functions, highlighting how physicality reads in comparison to the density matrix formalism. Wigner differential entropy was defined for nonnegative phase distributions. We presented different quantum optical states with particular properties. Pure loss channels were introduced in chapter 3. We addressed the origin of irreversibility in quantum mechanics. Lindblad equation was used to derive the evolution of Wigner distributions in pure loss channels.

In the second part of this report, we presented our contribution to a start of proof for the conjecture. Chapter 4 was dedicated to our analytic developments. We first explained the context of the conjecture. Then, we gave a scheme of demonstration to prove it. Our main contribution was the derivation of a majorization criterion. Under some conditions, this criterion ensures that a phase distriubtion is majorized by its output through a pure loss channel. We proposed several tracks that could lead to a complete proof. We conducted numerical simulations in chapter 5. Different methods to generate nonnegative physical phase distributions were presented. We gave several examples to show that the conjecture is respected. Finally, through numerical evidence we showed that decreasing rearrangements of physical Wigner distribution are not necessarily physical.

If one result should be retained from this report, it is without a doubt the majorization criterion. This result is impressive by the simplicity of its formulation. A thinkable hypothesis is that this criterion formulates another physicality condition on Wigner distributions. We dare hope that this constitutes a first step towards a simple expression of physicality in the phase space formalism.

Bibliography

[1] Stéphane Attal, Alain Joye, and Claude-Alain Pillet. *Open Quantum Systems II: The Markovian Approach*. Springer, 2006.

[2] Leslie E Ballentine. *Quantum mechanics: a modern development*. World Scientific Publishing Co Inc, 2014.

[3] Charles H Bennett and Gilles Brassard. Quantum cryptography: Public key distribution and coin tossing. 1984.

[4] Iwo Białynicki-Birula and Jerzy Mycielski. Uncertainty relations for information entropy in wave mechanics. *Communications in Mathematical Physics*, 44(2):129–132, 1975.

[5] Iwo Bialynicki-Birula and Łukasz Rudnicki. Entropic uncertainty relations in quantum physics. In *Statistical Complexity*, pages 1–34. Springer, 2011.

[6] Dik Bouwmeester, Jian-Wei Pan, Klaus Mattle, Manfred Eibl, Harald Weinfurter, and Anton Zeilinger. Experimental quantum teleportation. *Nature*, 390(6660):575–579, 1997.

[7] Carlos Alexandre Brasil, Felipe Fernandes Fanchini, and Reginaldo de Jesus Napolitano. A simple derivation of the lindblad equation. *Revista Brasileira de Ensino de Física*, 35(1):01–09, 2013.

[8] Heinz-Peter Breuer and Francesco Petruccione. *The theory of open quantum systems*. Oxford University Press on Demand, 2002.

[9] Almut Burchard. A short course on rearrangement inequalities. *Lecture notes, IMDEA Winter School, Madrid*, (June):1–47, 2009.

[10] William B Case. Wigner functions and weyl transforms for pedestrians. *American Journal of Physics*, 76(10):937–946, 2008.

[11] Thomas M Cover and Joy A Thomas. *Elements of information theory*. John Wiley & Sons, 2012.

[12] CN Gagatsos, Ognyan Oreshkov, and NJ Cerf. Majorization relations and entanglement generation in a beam splitter. *Physical Review A*, 87(4):042307, 2013.

[13] Anaelle Hertz, Michael G Jabbour, and Nicolas J Cerf. Entropy-power uncertainty relations: towards a tight inequality for all gaussian pure states. *arXiv preprint arXiv:1702.07286*, 2017.

[14] Robin L Hudson. When is the wigner quasi-probability density non-negative? *Reports on Mathematical Physics*, 6(2):249–252, 1974.

[15] Michael G Jabbour, Raúl García-Patrón, and Nicolas J Cerf. Majorization preservation of gaussian bosonic channels. *New Journal of Physics*, 18(7):073047, 2016.

[16] Young-Suk Kim and Marilyn E Noz. *Phase space picture of quantum mechanics: group theoretical approach*, volume 40. World Scientific, 1991.

[17] Peter Lambropoulos and David Petrosyan. *Fundamentals of quantum optics and quantum information*. Springer Science & Business Media, 2007.

[18] Rolf Landauer. The physical nature of information. *Physics letters A*, 217(4-5):188–193, 1996.

[19] Ulf Leonhardt. *Essential quantum optics: from quantum measurements to black holes*. Cambridge University Press, 2010.

[20] Elliott H. Lieb and Michael Loss. *Analysis*, volume 14. 2001.

[21] Leonard Mandel and Emil Wolf. *Optical coherence and quantum optics*. Cambridge university press, 1995.

[22] G Manfredi and MR Feix. Entropy and wigner functions. *Physical Review E*, 62(4):4665, 2000.

[23] Albert W. Marshall, Ingram Olkin, and Barry C. Arnold. *Inequalities: Theory of Majorization and Its Applications*. 2011.

[24] Klaus Mattle, Harald Weinfurter, Paul G Kwiat, and Anton Zeilinger. Dense coding in experimental quantum communication. *Physical Review Letters*, 76(25):4656, 1996.

[25] Michael Nielsen. An introduction to majorization and its applications to quantum mechanics. *Lecture Notes, Department of Physics, University ...*, 2002.

[26] Michael A Nielsen and Isaac Chuang. Quantum computation and quantum information, 2002.

[27] Jose C Principe. *Information theoretic learning: Renyi's entropy and kernel perspectives*. Springer Science & Business Media, 2010.

[28] A Wayne Roberts and Dale E Varberg. *Convex Functions*. Number 3. 1973.

[29] Gabor Szeg. *Orthogonal polynomials*, volume 23. American Mathematical Soc., 1939.

[30] Liyao Wang and Mokshay Madiman. Beyond the entropy power inequality, via rearrangements. *IEEE Transactions on Information Theory*, 60(9):5116–5137, 2014.

[31] Christian Weedbrook, Stefano Pirandola, Raúl García-Patrón, Nicolas J Cerf, Timothy C Ralph, Jeffrey H Shapiro, and Seth Lloyd. Gaussian quantum information. *Reviews of Modern Physics*, 84(2):621, 2012.

[32] William K Wootters and Wojciech H Zurek. A single quantum cannot be cloned. *Nature*, 299(5886):802–803, 1982.

[33] Cosmas Zachos, David Fairlie, and Thomas Curtright. *Quantum mechanics in phase space: an overview with selected papers*, volume 34. World Scientific, 2005.

Appendix A

Second quantization

In this appendix, we make a summary of the derivation that leads to the second quantization. Quantum optics is the physical background that we use in this report. Therefore, we consider useful to reminds the origin of the quantization of the electromagnetic field. We use mainly [21] and [17].

A.1 Classical Maxwell equations

The Maxwell equations in vacuum read

$$\begin{aligned} \nabla \times \mathbf{E} &= -\frac{\partial \mathbf{B}}{\partial t}, & \nabla \cdot \mathbf{E} &= 0, \\ \nabla \times \mathbf{B} &= \frac{1}{c^2}\frac{\partial \mathbf{E}}{\partial t}, & \nabla \cdot \mathbf{B} &= 0. \end{aligned} \tag{A.1.1}$$

$\mathbf{E}(\mathbf{r},t)$ is the electrical field and $\mathbf{B}(\mathbf{r},t)$ is the magnetic field. $c = (\epsilon_0\mu_0)^{-1/2}$ is the speed of light in vacuum, ϵ_0 is the vacuum permittivity and μ_0 is the vacuum permeability. Introducing the vector potential $\mathbf{A}(\mathbf{r},t)$ and the Coulomb gauge $\nabla\cdot\mathbf{A} = 0$, we can deduce both $\mathbf{E}$ and $\mathbf{B}$ from $\mathbf{A}$.

$$\mathbf{E} = -\frac{\partial \mathbf{A}}{\partial t}, \qquad \mathbf{B} = \nabla \times \mathbf{A} \tag{A.1.2}$$

Using these relations in A.1.1 leads us to the wave equation for the vector potential :

$$\left(\frac{1}{c^2}\frac{\partial^2}{\partial t^2} - \Delta\right)\mathbf{A} = 0 \tag{A.1.3}$$

We can restrict ourselves to the study of the vector potential. A common derivation leading to the second quantization consist in considering a large cube of volume V with periodic boundary conditions. Assuming this, we may expand $\mathbf{A}$ on the plane wave modes.

$$\mathbf{A}(\mathbf{r},t) = \sum_{\mathbf{k}\lambda} \left[A_{\mathbf{k}\lambda}(t)\mathbf{v}_{\mathbf{k}\lambda}(\mathbf{r}) + A^*_{\mathbf{k}\lambda}(t)\mathbf{v}^*_{\mathbf{k}\lambda}(\mathbf{r})\right] \tag{A.1.4}$$

where

$$A_{\mathbf{k}\lambda}(t) = \sqrt{\frac{\hbar}{2\epsilon_0\omega_{\mathbf{k}}}}\alpha_{\mathbf{k}\lambda}\exp(-\mathrm{i}\omega_{\mathbf{k}}t), \qquad \mathbf{v}_{\mathbf{k}\lambda} = \hat{\mathbf{e}}_{\mathbf{k}\lambda}\frac{\exp(\mathrm{i}\mathbf{k}\mathbf{r})}{\sqrt{V}} \tag{A.1.5}$$

The summation in A.1.4 is done over every possible mode. The index $\mathbf{k}$ browse all the possible wave vectors, and the index λ has two different values accounting for the

two possible orthogonal polarizations. $\omega_{\mathbf{k}}$ is linked to $\mathbf{k}$ through the dispersion relation : $\omega_{\mathbf{k}} = \|\mathbf{k}\|c$.

The relations A.1.5 are chosen according to the plane wave expansion. $\hat{\mathbf{e}}_{\mathbf{k}\lambda}$ is a unit vector such that $\hat{\mathbf{e}}_{\mathbf{k}\lambda} \cdot \hat{\mathbf{e}}_{\mathbf{k}\lambda'} = \delta_{\lambda\lambda'}$ and $\hat{\mathbf{e}}_{\mathbf{k}\lambda} \cdot \mathbf{k} = 0$. A dimensional prefactor is chosen in the temporal dependence, in order to show up the adimensional number $\alpha_{\mathbf{k}\lambda}$. The spatial modes are normalized : $\int_V \mathbf{v}^*_{\mathbf{k}\lambda}\mathbf{v}_{\mathbf{k}\lambda}\mathrm{d}^3\mathbf{r} = 1$.

We now introduce the quantities $q_{\mathbf{k}\lambda}$ and $p_{\mathbf{k}\lambda}$:

$$q_{\mathbf{k}\lambda} = \sqrt{\frac{\hbar}{2\omega_{\mathbf{k}}}}\left(\alpha_{\mathbf{k}\lambda} + \alpha^*_{\mathbf{k}\lambda}\right), \qquad p_{\mathbf{k}\lambda} = -\mathrm{i}\sqrt{\frac{\hbar\omega_{\mathbf{k}}}{2}}\left(\alpha_{\mathbf{k}\lambda} - \alpha^*_{\mathbf{k}\lambda}\right) \tag{A.1.6}$$

In light of these elements, we may calculate the total energy H in the field. Using the orthogonality of the spatial modes, we have :

$$H = \int_V \left(\frac{\epsilon_0}{2}\mathbf{E}^2 + \frac{1}{2\mu_0}\mathbf{B}^2\right)\mathrm{d}^3\mathbf{r} \tag{A.1.7a}$$

$$= \sum_{\mathbf{k}\lambda} \hbar\omega_{\mathbf{k}}|\alpha_{\mathbf{k}\lambda}|^2 \tag{A.1.7b}$$

$$= \frac{1}{2}\sum_{\mathbf{k}\lambda} \hbar\omega_{\mathbf{k}}\left(\alpha^*_{\mathbf{k}\lambda}\alpha_{\mathbf{k}\lambda} + \alpha_{\mathbf{k}\lambda}\alpha^*_{\mathbf{k}\lambda}\right) \tag{A.1.7c}$$

$$= \frac{1}{2}\sum_{\mathbf{k}\lambda} \left(\omega^2_{\mathbf{k}}q^2_{\mathbf{k}\lambda} + p^2_{\mathbf{k}\lambda}\right) \tag{A.1.7d}$$

A.2 Quantization

The quantum step can now happen if we notice that each mode of the electromagnetic field behaves like an harmonic oscillator. Having in mind the resolution of the harmonic oscillator, we replace $q_{\mathbf{k}\lambda}$ and $p_{\mathbf{k}\lambda}$ with the canonically conjugate operators $\hat{q}_{\mathbf{k}\lambda}$ and $\hat{p}_{\mathbf{k}\lambda}$. Conversely to A.1.6, we introduce the annihilation operator $\hat{a}_{\mathbf{k}\lambda}$ and creation operator $\hat{a}^\dagger_{\mathbf{k}\lambda}$.

$$\hat{a}_{\mathbf{k}\lambda} = \frac{1}{\sqrt{2\hbar\omega_{\mathbf{k}}}}\left(\omega_{\mathbf{k}}q_{\mathbf{k}\lambda} + \mathrm{i}p_{\mathbf{k}\lambda}\right), \qquad \hat{a}^\dagger_{\mathbf{k}\lambda} = \frac{1}{\sqrt{2\hbar\omega_{\mathbf{k}}}}\left(\omega_{\mathbf{k}}q_{\mathbf{k}\lambda} - \mathrm{i}p_{\mathbf{k}\lambda}\right) \tag{A.2.1}$$

These operators obey the following commutation rules :

$$\left[q_{\mathbf{k}\lambda}, p_{\mathbf{k}'\lambda'}\right] = \mathrm{i}\hbar\delta_{\mathbf{k}\mathbf{k}'}\delta_{\lambda\lambda'}, \qquad \left[q_{\mathbf{k}\lambda}, q_{\mathbf{k}'\lambda'}\right] = \left[p_{\mathbf{k}\lambda}, p_{\mathbf{k}'\lambda'}\right] = 0 \tag{A.2.2a}$$

$$\left[\hat{a}_{\mathbf{k}\lambda}, \hat{a}^\dagger_{\mathbf{k}'\lambda'}\right] = \delta_{\mathbf{k}\mathbf{k}'}\delta_{\lambda\lambda'}, \qquad \left[\hat{a}_{\mathbf{k}\lambda}, \hat{a}_{\mathbf{k}'\lambda'}\right] = \left[\hat{a}^\dagger_{\mathbf{k}\lambda}, \hat{a}^\dagger_{\mathbf{k}'\lambda'}\right] = 0 \tag{A.2.2b}$$

The quantum scalar potential operator $\hat{\mathbf{A}}$ is obtained from A.1.4 and A.1.5 where $\alpha_{\mathbf{k}\lambda}$ has been replaced with $\hat{a}_{\mathbf{k}\lambda}$. The quantum electrical field operator $\hat{\mathbf{E}}$ and the quantum magnetic field operator $\hat{\mathbf{B}}$ are then obtained from A.1.2.

We introduce the photon number operator $\hat{N}_{\mathbf{k}\lambda} = \hat{a}^\dagger_{\mathbf{k}\lambda}\hat{a}_{\mathbf{k}\lambda}$. Using equation A.1.7c and the commutation rules that we established, the total field energy operator may write :

$$\hat{H} = \sum_{\mathbf{k}\lambda} \hbar\omega_{\mathbf{k}}\left(\hat{N}_{\mathbf{k}\lambda} + \frac{1}{2}\right) \tag{A.2.3}$$

Appendix B

Evolution of Wigner distributions in a pure loss channel

In this appendix, we derive the evolution of a WDF evolving in a PLC.

B.1 Correspondence rules

First, we derive the correspondence rules which give us the effect of the operator $\hat{q}$ and $\hat{p}$ on the WDF. Hereafter, we explict the derivation proposed in [19].

Let W be the WDF associated to the state $\hat{\rho}$, and $W_{\hat{q}\hat{\rho}}$ the WDF associated to the state $\hat{q}\hat{\rho}$.

$$\begin{aligned} W_{\hat{q}\hat{\rho}} &= \frac{1}{2\pi}\int_{-\infty}^{+\infty} \exp(ipx)\left\langle q-\frac{x}{2}\right|\hat{q}\hat{\rho}\left|q+\frac{x}{2}\right\rangle \mathrm{d}x \\ &= \frac{1}{2\pi}\int_{-\infty}^{+\infty} \exp(ipx)\left(q-\frac{x}{2}\right)\left\langle q-\frac{x}{2}\right|\hat{\rho}\left|q+\frac{x}{2}\right\rangle \mathrm{d}x \\ &= \left(q+\frac{i}{2}\frac{\partial}{\partial p}\right)\frac{1}{2\pi}\int_{-\infty}^{+\infty} \exp(ipx)\left\langle q-\frac{x}{2}\right|\hat{\rho}\left|q+\frac{x}{2}\right\rangle \mathrm{d}x \\ &= \left(q+\frac{i}{2}\frac{\partial}{\partial p}\right) W \end{aligned} \tag{B.1.1}$$

For $W_{\hat{\rho}\hat{q}}$ we have similarly :

$$\begin{aligned} W_{\hat{\rho}\hat{q}} &= \frac{1}{2\pi}\int_{-\infty}^{+\infty} \exp(ipx)\left\langle q-\frac{x}{2}\right|\hat{\rho}\hat{q}\left|q+\frac{x}{2}\right\rangle \mathrm{d}x \\ &= \frac{1}{2\pi}\int_{-\infty}^{+\infty} \exp(ipx)\left\langle q-\frac{x}{2}\right|\hat{\rho}\left|q+\frac{x}{2}\right\rangle \left(q+\frac{x}{2}\right) \mathrm{d}x \\ &= \left(q-\frac{i}{2}\frac{\partial}{\partial p}\right)\frac{1}{2\pi}\int_{-\infty}^{+\infty} \exp(ipx)\left\langle q-\frac{x}{2}\right|\hat{\rho}\left|q+\frac{x}{2}\right\rangle \mathrm{d}x \\ &= \left(q-\frac{i}{2}\frac{\partial}{\partial p}\right) W \end{aligned} \tag{B.1.2}$$

To compute $W_{\hat{p}\hat{\rho}}$, we use the definition of W in the momentum basis :

$$\begin{aligned} W_{\hat{p}\hat{\rho}} &= \frac{1}{2\pi}\int_{-\infty}^{+\infty} \exp(iqy)\left\langle p+\frac{y}{2}\right|\hat{p}\hat{\rho}\left|p-\frac{y}{2}\right\rangle \mathrm{d}y \\ &= \frac{1}{2\pi}\int_{-\infty}^{+\infty} \exp(iqy)\left(p+\frac{y}{2}\right)\left\langle p+\frac{y}{2}\right|\hat{\rho}\left|p-\frac{y}{2}\right\rangle \mathrm{d}y \\ &= \left(p-\frac{i}{2}\frac{\partial}{\partial q}\right)\frac{1}{2\pi}\int_{-\infty}^{+\infty} \exp(iqy)\left\langle p+\frac{y}{2}\right|\hat{\rho}\left|p-\frac{y}{2}\right\rangle \mathrm{d}y \\ &= \left(p-\frac{i}{2}\frac{\partial}{\partial q}\right) W \end{aligned} \tag{B.1.3}$$

Similarly for $W_{\hat{\rho}\hat{p}}$, we have :

$$\begin{aligned} W_{\hat{\rho}\hat{p}} &= \frac{1}{2\pi}\int_{-\infty}^{+\infty} \exp(iqy)\left\langle p+\frac{y}{2}\right|\hat{\rho}\hat{p}\left|p-\frac{y}{2}\right\rangle \mathrm{d}y \\ &= \frac{1}{2\pi}\int_{-\infty}^{+\infty} \exp(iqy)\left\langle p+\frac{y}{2}\right|\hat{\rho}\left|p-\frac{y}{2}\right\rangle \left(p-\frac{y}{2}\right) \mathrm{d}y \\ &= \left(p+\frac{i}{2}\frac{\partial}{\partial q}\right)\frac{1}{2\pi}\int_{-\infty}^{+\infty} \exp(iqy)\left\langle p+\frac{y}{2}\right|\hat{\rho}\left|p-\frac{y}{2}\right\rangle \mathrm{d}y \\ &= \left(p+\frac{i}{2}\frac{\partial}{\partial q}\right) W \end{aligned} \tag{B.1.4}$$

Brought back together, these four relations give the following correspondence rules:

$$\boxed{\begin{array}{ll} \hat{q}\hat{\rho} \leftrightarrow \left(q+\frac{i}{2}\frac{\partial}{\partial p}\right) W & \hat{\rho}\hat{q} \leftrightarrow \left(q-\frac{i}{2}\frac{\partial}{\partial p}\right) W \\ \hat{p}\hat{\rho} \leftrightarrow \left(p-\frac{i}{2}\frac{\partial}{\partial q}\right) W & \hat{\rho}\hat{p} \leftrightarrow \left(p+\frac{i}{2}\frac{\partial}{\partial q}\right) W \end{array}} \tag{B.1.5}$$

B.2 Lindblad equation for the WDF

Now, we derive the evolution equation of the WDF. We start from the evolution equation of the density matrix in a PLC :

$$\boxed{\frac{\mathrm{d}\hat{\rho}}{\mathrm{d}t} = \Gamma\left(\hat{a}\hat{\rho}\hat{a}^\dagger - \frac{1}{2}\hat{a}^\dagger\hat{a}\hat{\rho} - \frac{1}{2}\hat{\rho}\hat{a}^\dagger\hat{a}\right)} \tag{B.2.1}$$

We remember the definition of $\hat{a}$ and $\hat{a}^\dagger$ in terms of $\hat{q}$ and $\hat{p}$:

$$\hat{a} = \frac{1}{\sqrt{2}}(\hat{q} + i\hat{p}), \qquad \hat{a}^\dagger = \frac{1}{\sqrt{2}}(\hat{q} - i\hat{p}). \tag{B.2.2}$$

We can rewrite B.2.1 as :

$$\begin{aligned}\frac{1}{\Gamma}\frac{\partial\hat{\rho}}{\partial t} &= \hat{a}\hat{\rho}\hat{a}^\dagger - \frac{1}{2}\hat{a}^\dagger\hat{a}\hat{\rho} - \frac{1}{2}\hat{\rho}\hat{a}^\dagger\hat{a} \\ &= \frac{1}{2}(\hat{q}+i\hat{p})\hat{\rho}(\hat{q}-i\hat{p}) - \frac{1}{4}(\hat{q}-i\hat{p})(\hat{q}+i\hat{p})\hat{\rho} - \frac{1}{4}\hat{\rho}(\hat{q}-i\hat{p})(\hat{q}+i\hat{p}) \\ &= \frac{1}{2}\left(\hat{q}\hat{\rho}\hat{q} + \hat{p}\hat{\rho}\hat{p} + i\hat{p}\hat{\rho}\hat{q} - i\hat{q}\hat{\rho}\hat{p}\right) - \frac{1}{4}\left(\hat{q}^2+\hat{p}^2-1\right)\hat{\rho} - \frac{1}{4}\hat{\rho}\left(\hat{q}^2+\hat{p}^2-1\right)\end{aligned} \tag{B.2.3}$$

where we have used the commutation relation $[\hat{q},\hat{p}] = i$.

The latter equation may seem quite stodgy, but it actually leads to the evolution equation of the WDF in a PLC. In order to do so, we use the previously derived correspondence rules. We translate the evolution equation of the density matrix to the evolution equation of the WDF.

$$\begin{aligned}\frac{1}{\Gamma}\frac{\partial W}{\partial t} &= \frac{1}{2}\left(\left(q+\frac{i}{2}\frac{\partial}{\partial p}\right)\left(q-\frac{i}{2}\frac{\partial}{\partial p}\right) + \left(p-\frac{i}{2}\frac{\partial}{\partial q}\right)\left(p+\frac{i}{2}\frac{\partial}{\partial q}\right)\right)W \\ &+ \frac{i}{2}\left(\left(p-\frac{i}{2}\frac{\partial}{\partial q}\right)\left(q-\frac{i}{2}\frac{\partial}{\partial p}\right) - \left(q+\frac{i}{2}\frac{\partial}{\partial p}\right)\left(p+\frac{i}{2}\frac{\partial}{\partial q}\right)\right)W \\ &- \frac{1}{4}\left(\left(q+\frac{i}{2}\frac{\partial}{\partial p}\right)^2 + \left(q-\frac{i}{2}\frac{\partial}{\partial p}\right)^2 + \left(p+\frac{i}{2}\frac{\partial}{\partial q}\right)^2 + \left(p-\frac{i}{2}\frac{\partial}{\partial q}\right)^2 - 2\right)W\end{aligned} \tag{B.2.4}$$

Fortunately, the previous equation can be simplified to :

$$\begin{aligned}\frac{1}{\Gamma}\frac{\partial W}{\partial t} &= \frac{1}{2}\left(q^2+p^2+\frac{1}{4}\frac{\partial^2}{\partial p^2}+\frac{1}{4}\frac{\partial^2}{\partial q^2}\right)W \\ &+ \frac{1}{2}\left(\frac{1}{2}q\frac{\partial}{\partial q}+\frac{1}{2}p\frac{\partial}{\partial p}+\frac{1}{2}\frac{\partial}{\partial q}q+\frac{1}{2}\frac{\partial}{\partial p}p\right)W \\ &- \frac{1}{4}\left(2q^2+2p^2-\frac{1}{2}\frac{\partial^2}{\partial q^2}-\frac{1}{2}\frac{\partial^2}{\partial p^2}-2\right)W\end{aligned} \tag{B.2.5}$$

So that it finally resumes to :

$$\boxed{\frac{\partial W}{\partial t} = \frac{\Gamma}{2}\left(2+q\frac{\partial}{\partial q}+p\frac{\partial}{\partial p}+\frac{1}{2}\frac{\partial^2}{\partial q^2}+\frac{1}{2}\frac{\partial^2}{\partial p^2}\right)W} \tag{B.2.6}$$

B.3 Lindblad equation for the characteristic function

In this section we compute the evolution equation of the characteristic function $\tilde{W}(u,v)$. To do so, we investigate how equation B.2.6 translates to the characteristic function. Let us consider the following relations :

$$\frac{\partial}{\partial u}\int_{-\infty}^{+\infty}\int_{-\infty}^{+\infty} W(q,p)\exp(-iuq-ivp)\mathrm{d}q\mathrm{d}p = -i\int_{-\infty}^{+\infty}\int_{-\infty}^{+\infty} qW(q,p)\exp(-iuq-ivp)\mathrm{d}q\mathrm{d}p \tag{B.3.1a}$$

$$\frac{\partial}{\partial v}\int_{-\infty}^{+\infty}\int_{-\infty}^{+\infty} W(q,p)\exp(-iuq-ivp)\mathrm{d}q\mathrm{d}p = -i\int_{-\infty}^{+\infty}\int_{-\infty}^{+\infty} pW(q,p)\exp(-iuq-ivp)\mathrm{d}q\mathrm{d}p \tag{B.3.1b}$$

$$\frac{\partial}{\partial q}\int_{-\infty}^{+\infty}\int_{-\infty}^{+\infty} \tilde{W}(u,v)\exp(iuq+ivp)\mathrm{d}u\mathrm{d}v = i\int_{-\infty}^{+\infty}\int_{-\infty}^{+\infty} u\tilde{W}(u,v)\exp(iuq+ivp)\mathrm{d}u\mathrm{d}v \tag{B.3.1c}$$

$$\frac{\partial}{\partial p}\int_{-\infty}^{+\infty}\int_{-\infty}^{+\infty} \tilde{W}(u,v)\exp(iuq+ivp)\mathrm{d}u\mathrm{d}v = i\int_{-\infty}^{+\infty}\int_{-\infty}^{+\infty} v\tilde{W}(u,v)\exp(iuq+ivp)\mathrm{d}u\mathrm{d}v \tag{B.3.1d}$$

$$\boxed{\begin{array}{ll} qW \leftrightarrow i\dfrac{\partial}{\partial u}\tilde{W} & pW \leftrightarrow i\dfrac{\partial}{\partial v}\tilde{W} \\ \dfrac{\partial}{\partial q}W \leftrightarrow iu\tilde{W} & \dfrac{\partial}{\partial p}W \leftrightarrow iv\tilde{W} \end{array}} \tag{B.3.2}$$

We now inject this in equation B.2.6 and get the following result:

$$\frac{\partial\tilde{W}}{\partial t} = \frac{\Gamma}{2}\left(2 - \frac{\partial}{\partial u}u - \frac{\partial}{\partial v}v - \frac{1}{2}u^2 - \frac{1}{2}v^2\right)\tilde{W} \tag{B.3.3}$$

$$\boxed{\frac{\partial\tilde{W}}{\partial t} = -\frac{\Gamma}{2}\left(u\frac{\partial}{\partial u} + v\frac{\partial}{\partial v} + \frac{1}{2}u^2 + \frac{1}{2}v^2\right)\tilde{W}} \tag{B.3.4}$$

B.4 Evolution of the characteristic function

Here, we show the explicit expression of the characteristic function. The solution of the evolution equation B.3.4 has the following form:

$$\boxed{\tilde{W}(u,v,t) = \tilde{W}^{(\mathrm{in})}\left(u\sqrt{\eta}, v\sqrt{\eta}\right)\exp\left((\eta-1)\frac{u^2+v^2}{4}\right)} \tag{B.4.1}$$

where $\eta = \exp(-\Gamma t)$ and $\tilde{W}^{(\mathrm{in})}(u,v)$ is the characteristic function at $t=0$. As a proof, we calculate calculate explicitly that it verifies the evolution equation. For readability, we introduce the following variables u' and v':

$$u' = u\sqrt{\eta}, \qquad v' = v\sqrt{\eta}. \tag{B.4.2}$$

B.4.1 Temporal dependence

First we calculate $\frac{\partial}{\partial t}\tilde{W}(u,v,t)$. Using the relation

$$\frac{\partial}{\partial t}F\left(x(t),y(t)\right)=\frac{\partial F}{\partial x}\frac{\partial}{\partial t}x(t)+\frac{\partial W}{\partial y}\frac{\partial}{\partial t}y(t) \tag{B.4.3}$$

and the notation

$$\tilde{W}'^{u}(u,v)=\frac{\partial\tilde{W}}{\partial u}(u,v) \qquad\qquad \tilde{W}'^{v}(u,v)=\frac{\partial\tilde{W}}{\partial v}(u,v) \tag{B.4.4}$$

We have :

$$\frac{\partial}{\partial t}\tilde{W}_0\left(u',v'\right)=-\frac{\Gamma}{2}\sqrt{\eta}\left(u\tilde{W}_0'^{u}\left(u',v'\right)+v\tilde{W}_0'^{v}\left(u',v'\right)\right) \tag{B.4.5}$$

$$\begin{aligned}\frac{\partial}{\partial t}\tilde{W}(u,v,t)=&-\frac{\Gamma}{2}\sqrt{\eta}\left(u\tilde{W}_0'^{u}\left(u',v'\right)+v\tilde{W}_0'^{v}\left(u',v'\right)\right)\exp\left((\eta-1)\frac{u^2+v^2}{4}\right)\\&-\Gamma\eta\left(\frac{u^2+v^2}{4}\right)\exp\left((\eta-1)\frac{u^2+v^2}{4}\right)\tilde{W}_0\left(u',v'\right)\end{aligned} \tag{B.4.6}$$

B.4.2 Coordinate dependence

We are now going to calculate $-\frac{\Gamma}{2}\left(u\frac{\partial}{\partial u}+v\frac{\partial}{\partial v}+\frac{1}{2}u^2+\frac{1}{2}v^2\right)\tilde{W}(u,v,t)$ and verify that it is indeed equal to $\frac{\partial}{\partial t}\tilde{W}(u,v,t)$.

$$\frac{\partial}{\partial u}\tilde{W}(u,v,t)=\exp\left((\eta-1)\frac{u^2+v^2}{4}\right)\left((\eta-1)\frac{u}{2}\tilde{W}_0\left(u',v'\right)\sqrt{\eta}\tilde{W}_0'^{u}\left(u',v'\right)\right) \tag{B.4.7}$$

$$\frac{\partial}{\partial v}\tilde{W}(u,v,t)=\exp\left((\eta-1)\frac{u^2+v^2}{4}\right)\left((\eta-1)\frac{v}{2}\tilde{W}_0\left(u',v'\right)\sqrt{\eta}\tilde{W}_0'^{v}\left(u',v'\right)\right) \tag{B.4.8}$$

Finally, we have :

$$\begin{aligned}-\frac{\Gamma}{2}\left(u\frac{\partial}{\partial u}+v\frac{\partial}{\partial v}+\frac{1}{2}u^2+\frac{1}{2}v^2\right)\tilde{W}(u,v,t)=&-\frac{\Gamma}{2}\exp\left((\eta-1)\frac{u^2+v^2}{4}\right)\\&\times\left(\eta\frac{u^2+v^2}{2}\tilde{W}_0\left(u',v'\right)+u\sqrt{\eta}\tilde{W}_0'^{u}\left(u',v'\right)+v\sqrt{\eta}\tilde{W}_0'^{v}\left(u',v'\right)\right)\end{aligned} \tag{B.4.9}$$

Obviously, equations B.4.6 and B.4.9 are equal.

B.5 Evolution of the WDF

We see from equation B.4.1 that the evolution of the characteristic function in governed by two different mechanisms. $\tilde{W}^{(\mathrm{in})}(u,v)$ first undergoes a rescaling, and is then multiplied

with a Gaussian. The multiplication in Fourier space corresponds to a convolution in real space.

We introduce the function $\tilde{G}_\eta$ as :

$$\tilde{G}_\eta(u,v) = \exp\left((\eta-1)\frac{u^2+v^2}{4}\right) \tag{B.5.1}$$

so that $W(q,p,t)$ can be expressed as :

$$\begin{aligned} W(q,p,t) &= \mathrm{FT}^{-1}\left[\tilde{W}(u,v,t)\right] \\ &= \mathrm{FT}^{-1}\left[\tilde{W}^{(\mathrm{in})}(u\sqrt{\eta},v\sqrt{\eta})\cdot\tilde{G}_\eta\right] \\ &= \mathrm{FT}^{-1}\left[\tilde{W}^{(\mathrm{in})}(u\sqrt{\eta},v\sqrt{\eta})\right] * \mathrm{FT}^{-1}\left[\tilde{G}_\eta\right] \end{aligned} \tag{B.5.2}$$

B.5.1 Rescaling

Let us introduce the norm preserving rescaling operator R_s :

$$R_s\left[A(x,y)\right] = \frac{1}{s^2}A\left(\frac{x}{s},\frac{y}{s}\right) \tag{B.5.3}$$

$$\begin{aligned} \mathrm{FT}^{-1}\left[\tilde{W}^{(\mathrm{in})}(u\sqrt{\eta},v\sqrt{\eta})\right] &= \frac{1}{4\pi^2}\int_{-\infty}^{+\infty}\int_{-\infty}^{+\infty}\tilde{W}^{(\mathrm{in})}\left(u\sqrt{\eta},v\sqrt{\eta}\right)\exp(iuq+ivp)\mathrm{d}u\mathrm{d}v \\ &= \frac{1}{\eta}\frac{1}{4\pi^2}\int_{-\infty}^{+\infty}\int_{-\infty}^{+\infty}\tilde{W}^{(\mathrm{in})}(u',v')\exp\left(iu'\frac{q}{\sqrt{\eta}}+iv'\frac{p}{\sqrt{\eta}}\right)\mathrm{d}u'\mathrm{d}s' \\ &= \frac{1}{\eta}W^{(\mathrm{in})}\left(\frac{q}{\sqrt{\eta}},\frac{p}{\sqrt{\eta}}\right) = R_{\sqrt{\eta}}\left[W^{(\mathrm{in})}(q,p)\right] \end{aligned} \tag{B.5.4}$$

B.5.2 Convolution

In real space, the rescaled WDF is convoluted with the inverse transform of $\tilde{G}_\eta(u,v)$. Hereafter, we compute the real function $G_\eta(q,p)$.

$$\begin{aligned} G_\eta = \mathrm{FT}^{-1}\left[\tilde{G}_\eta\right] &= \frac{1}{4\pi^2}\int_{-\infty}^{+\infty}\int_{-\infty}^{+\infty}\exp\left((\eta-1)\frac{u^2+v^2}{4}\right)\exp\left(iuq+ivp\right)\mathrm{d}u\mathrm{d}v \\ &= \frac{1}{\pi}\frac{1}{1-\eta}\exp\left(-\frac{q^2+p^2}{1-\eta}\right) \\ &= R_{\sqrt{1-\eta}}\left[\frac{1}{\pi}\exp\left(-q^2-p^2\right)\right] = R_{\sqrt{1-\eta}}\left[W_0(q,p)\right] \end{aligned} \tag{B.5.5}$$

where W_0 is the WDF of the vacuum.

B.5.3 Evolution of the WDF

The evolution of the WDF in a PLC is now fully determined. It can be expressed on the short form :

$$\boxed{W^{(\text{out})} = R_{\sqrt{\eta}}\left[W^{(\text{in})}\right] * R_{\sqrt{1-\eta}}\left[W_0\right]} \tag{B.5.6}$$

where the time dependence is included in $\eta = \exp(-\Gamma t)$, $W^{(\text{out})}$ is the WDF at time t, $W^{(\text{in})}$ is the WDF at $t = 0$ and W_0 is the WDF of vacuum.

It has the following explicit form :

$$\boxed{W^{(\text{out})}(q,p) = \frac{1}{\pi(1-\eta)} \int_{-\infty}^{+\infty}\int_{-\infty}^{+\infty} W^{(\text{in})}(q',p') \exp\left(-\frac{(q-\sqrt{\eta}q')^2 + (p-\sqrt{\eta}p')^2}{1-\eta}\right) \mathrm{d}q'\mathrm{d}p'} \tag{B.5.7}$$

Appendix C

Bell shaped functions

C.1 1D Bell shaped functions

Definition C.1. *Function $f(x)$ is a bell shaped function if and only if :*

$$\begin{cases} f(x) = f(-x) & \text{(C.1.1a)} \\ f'(x) \leq 0 \quad \text{if } x \geq 0 & \text{(C.1.1b)} \end{cases}$$

Lemma C.1. *The convolution of two bell shaped functions is a bell shaped function.*

Proof. Let f, g be bell shaped functions and $h = f * g$. To be a bell shaped function, h must satisfy and C.1.1a and C.1.1b. The proof of C.1.1a is straightforward :

$$h(-x) = \int_{-\infty}^{+\infty} f(t)g(-x-t)\mathrm{d}t = \int_{-\infty}^{+\infty} f(-t)g(x+t)\mathrm{d}t = \int_{-\infty}^{+\infty} f(t')g(x-t')\mathrm{d}t' = h(x) \tag{C.1.2}$$

To prove C.1.1b, we calculate the sign of $h'(x)$:

$$\begin{aligned} h'(x) &= \int_{-\infty}^{+\infty} f(t)g'(x-t)\mathrm{d}t = \int_{-\infty}^{+\infty} g'(t)f(x-t)\mathrm{d}t \\ &= \int_{0}^{+\infty} g'(t)f(x-t)\mathrm{d}t + \int_{0}^{+\infty} g'(-t)f(x+t)\mathrm{d}t \end{aligned} \tag{C.1.3}$$

From the definition C.1.1a, it is easily seen that $f'(-x) = -f'(x)$ and $g'(-x) = -g(x)$. We have :

$$h'(x) = \int_{0}^{+\infty} \underbrace{g'(t)}_{\leq 0} \left[f(x-t) - f(x+t)\right] \mathrm{d}t \tag{C.1.4}$$

We are now going to prove that $[f(x-t) - f(x+t)] \geq 0$ if $x \geq 0$. Let's rewrite $[f(x-t) - f(x+t)]$ as a function of f' :

$$f(x-t) - f(x+t) = -\int_{x-t}^{x+t} f'(z)\mathrm{d}z \tag{C.1.5a}$$

$$= -\int_{t-x}^{t+x} f'(z)\mathrm{d}z \tag{C.1.5b}$$

where we have use the fact that $f'(-x) = -f'(x)$.

If $x \geq t$, it appears from the equality C.1.5a and C.1.1b that $f(x-t) - f(x+t) \geq 0$. If $0 \leq x \leq t$, it appears from the equality C.1.5b and C.1.1b that $f(x-t) - f(x+t) \geq 0$. We see that when $x \geq 0$, $f(x-t) - f(x+t) \geq 0$. From equation C.1.4, we conclude that $h'(x) \leq 0$ if $x \geq 0$. Since h satisfies C.1.1a and C.1.1b, h is a bell shaped function.

□

C.2 2D Bell shaped functions

Definition C.2. *Function $f(x,y)$ is a 2D bell shaped function if and only if :*

$$\begin{cases} f(x,y) = f_r(r) \quad \textit{where } r = \sqrt{x^2+y^2} & \text{(C.2.1a)} \\ f_r(r) \textit{ is a bell shaped function} & \text{(C.2.1b)} \end{cases}$$

Lemma C.2. *The convolution of two 2-D bell shaped functions is a 2-D bell shaped function.*

Proof. Let f, g be 2-D bell shaped functions and $h = f * g$.

$$h(x,y) = \iint_{-\infty}^{+\infty} f(u,v)g(x-u, y-v)\mathrm{d}u\mathrm{d}v \tag{C.2.2}$$

For symmetry reasons, it is clear that h must satisfy C.2.1a, so that $h(x,y) = h_r(r)$. Since $h(x,0) = h_r(x)$, we can restrict ourselves to prove that $h(x,0)$ is a bell shaped function.

$$\begin{aligned} h(x,0) &= \int_{-\infty}^{+\infty} \left[\int_{-\infty}^{+\infty} f(u,v)g(x-u,-v)\mathrm{d}u \right] \mathrm{d}v \\ &= \int_{-\infty}^{+\infty} \left[\int_{-\infty}^{+\infty} f_v(u)g_{-v}(x-u)\mathrm{d}u \right] \mathrm{d}v \\ &= \int_{-\infty}^{+\infty} \left[f_v * g_{-v} \right](x)\mathrm{d}v \end{aligned} \tag{C.2.3}$$

where $f_y(x)$ is another writing of $f(x,y)$.

We now prove that if $f(x,y)$ is a 2-D bell shaped function, $f_y(x)$ is a bell shaped function. We study $f_y(-x)$ and $f'_y(x)$:

$$f_y(-x) = f_r\left(\sqrt{(-x)^2+y^2}\right) = f_r\left(\sqrt{x^2+y^2}\right) = f_y(x) \tag{C.2.4a}$$

$$f'_y(x) = \frac{\partial}{\partial x} f_r\left(\sqrt{x^2+y^2}\right) = \underbrace{f'_r\left(\sqrt{x^2+y^2}\right)}_{\leq 0} \frac{x}{\sqrt{x^2+y^2}} \leq 0 \quad \text{if } x \geq 0 \tag{C.2.4b}$$

Since $f_y(x)$ satisfies C.2.4a and C.2.4b, $f_y(x)$ is a bell shaped function. The same argument is used for $g_y(x)$. By lemma C.1, $h_v = f_v * g_{-v}$ is a bell shaped function. We can write C.2.3 as :

$$h(x,0) = \int_{-\infty}^{+\infty} h_v(x)\mathrm{d}v \tag{C.2.5}$$

We see that $h(x,0)$ is an integral of bell shaped functions. By linearity of the derivative, the sum of bell shaped functions is a bell shaped function. Therefore, $h(x,0) = h_r(x)$ is a bell shaped function. Since h satisfies C.2.1a and C.2.1b, h is a 2-D bell shaped function. □

Appendix D

Matlab codes

D.1 Generation of Wigner distributions

D.1.1 fx_fock.m

```
function y = fx_fock(n,x)
%Gives the wave function of the nth Fock state at position x
y = exp(-x.^2/2).*hermiteH(n,x)/(pi^(1/4)*2^(n/2)*sqrt(factorial(n)));
end
```

D.1.2 fx_fock_sup.m

```
function f = fx_fock_sup(D,x)
%Gives the wave function of a superposition of Fock states at ...
   position x
%D is the list of each complex amplitude
D = D/sqrt(sum(abs(D).^2));
f = zeros(size(x));
for i=1:length(D)
    if D(i)~=0
        f=f+D(i)*fx_fock(i-1,x);
    end
end
f = f/sqrt(trapz(x,abs(f).^2));
end
```

D.1.3 weyl_trans.m

```
function W = weyl_trans(f,nr,rL,int)
%Computes the Weyl transform of the wave function f
dxdp = (rL/nr)^2;
g = linspace(-rL/2,rL/2,nr); %intervalles grille
[X,P] = meshgrid(g);
W=zeros(nr);
dint = (max(int)-min(int))/(length(int)-1);
```

```
for i=1:nr
    for j=1:nr
        x = X(i,j);
        p = P(i,j);
        W(i,j) = (dint/pi) *sum(real(exp(-2*1i*p*int) ...
            .*interp1(int,f,x-int,'spline',0) ...
            .*conj(interp1(int,f,x+int,'spline',0))));
    end
end
```

D.1.4 wig_fock.m

```
function W = wig_fock(n,nr,rL)
%Computes the WDF of the Fock state n
g = linspace(-rL/2,rL/2,nr);
[X,P] = meshgrid(g);
W = (1/pi)*(-1)^n*laguerreL(n,2*X.^2+2*P.^2).*exp(-X.^2-P.^2);
end
```

D.1.5 wig_fock_mix.m

```
function W = wig_fock_mix(D,nr,rL)
%Gives the WDF of a mixture of Fock states
D = D/sum(D);
W = zeros(nr);
for i=1:length(D)
    if(D(i)~=0)
        W = W+D(i)*wig_fock(i-1,nr,rL);
    end
end
end
```

D.1.6 wig_pass_extr.m

```
function W = wig_pass_extr(n,nr,rL)
%Gives the WDF of the nth extremal passive state
dxdp = (rL/nr)^2;
W = zeros(nr);
for i=0:n
    W = W+wig_fock(i,nr,rL);
end
W = W/(n+1);
end
```

D.1.7 wig_fock_sup.m

```
function W = wig_fock_sup(D,nr,rL,int)
%Computes the WDF for a superposition of Fock states
f = fx_fock_sup(D,int);
W = weyl_trans(f,nr,rL,int);
end
```

D.1.8 wig_coh.m

```
function W = wig_coh(n,nr,rL,a,s)
%Computes the Wigner function of the displaced nth Fock states with ...
    parameter a
if(nargin==4)
    s=1;
end
dx = sqrt(2)*real(a);
dp = sqrt(2)*imag(a);
g = linspace(-rL/2,rL/2,nr);
[X,P] = meshgrid(g);
X = X-dx;
P = P-dp;
W = (1/s^2) *(1/pi) *(-1)^n*laguerreL(n,(2*X.^2+2*P.^2)/s^2) ...
    .*exp((-X.^2-P.^2)/s^2);
end
```

D.1.9 rad_fock.m

```
function [f,r] = rad_fock(n,nr,rL)
%Gives the radial function of the nth Fock state
r = linspace(0,rL,nr);
f = laguerreL(n,2*r.^2).*exp(-r.^2);
f = (-1)^n*f/pi;
end
```

D.1.10 rad_fock_mix.m

```
function [f,r] = rad_fock_mix(D,nr,rL)
%Computes the radial function of a mixture of Fock states
D = D/sum(D);
r = linspace(0,rL,nr);
f = zeros(1,length(r));
for i=1:length(D)
    if D(i) ~= 0
        [fi,ri] = rad_fock(i-1,nr,rL);
        f = f + D(i)*fi;
    end
end
end
```

D.2 Pure loss channel

D.2.1 conv_gauss.m

```
function Wg = conv_gauss(W,rL,sigma)
%Wg is the result of the convolution of a Gaussian with parameter ...
    sigma and
%matrix W
if(nargin==2)
    sigma = 1;
end
if(sigma ~= 0)
    nr = length(W);
    dxdp = (rL/nr)^2;
    g = -linspace(-rL,rL,2*nr+1);
    [X,P] = meshgrid(g);
    gauss = dxdp*exp(-(X.^2+P.^2)/sigma^2)/(sigma^2*pi);
    Wg = conv2(W,gauss,'same');
else
    Wg = W;
end
```

D.2.2 rescale_mat.m

```
function Ws = rescale_mat(W,s,interp)
%Contracts matrix W with a factor s
%interp determines the type of interpolation
if nargin == 2
    interp = 'spline';
end
nr = length(W);
[X,Y] = meshgrid(linspace(-1/2,1/2,nr));
Xr = X*s;
Yr = Y*s;
Ws = interp2(X,Y,W,Xr,Yr,interp,0);
Ws(isnan(Ws))=0;
end
```

D.2.3 plc.m

```
function Wplc = plc(W,rL,eta)
%Gives the result of W passing through a PLC of parameter eta
nr = length(W);
dxdp = (rL/nr)^2;
if(nargin == 2)
    eta = 1/2;
end
if(eta == 0)
    Wplc = wig_fock(0,nr,rL);
elseif(eta == 1)
```

```
    Wplc = W;
else
    W = rescale_mat(W,sqrt(1/eta))/eta;
    Wplc = conv_gauss(W,rL,sqrt(1-eta));
end
end
```

D.2.4 plc_rad.m

```
function [Fc,Fint] = plc_rad(F,Fint,eta)
%Gives the radial function after passing through a PLC of parameter eta
Fc = zeros(size(F));
R = Fint;
for i=1:length(Fint)
    r = Fint(i);
    tot = F .*exp(-eta*R.^2/(1-eta)) ...
        .*besseli(0,(2*sqrt(eta)*r.*R)/(1-eta)).*R;
    Fc(i) = (2/(1-eta))*trapz(R,tot)*exp(-r^2/(1-eta));
end
end
```

D.3 Other functions

D.3.1 distr_phase.m

```
function D = distr_phase(n)
%Generates a distribution of n complex numbers, with equal modulus ...
    and random phases
%The distribution is normalized
D = zeros(1,n);
for i = 1:n
    D(i) = exp(1i*2*pi*rand);
end
D = D/sqrt(n);
end
```

D.3.2 distr_compl.m

```
function D = distr_compl(n)
%Generates a distribution of n complex numbers, with random phases and
%amplitudes
%The distribution is normalized
D = zeros(1,n);
for i = 1:n
    D(i) = rand*exp(1i*2*pi*rand);
end
D = D/sqrt(sum(abs(D).^2));
end
```

D.3.3 integ_mat.m

```
function int = integ_mat(W,dxdp)
%Evaluates the volume under the surface determined by W
n = length(W);
x = linspace(0,n,n);
int = trapz(x,trapz(x,W))*dxdp;
```

D.3.4 H.m

```
function H = H(W,dxdp,alpha)
% Evaluates Renyi entropy of parameter alpha for W
% Computes Wigner entropy if alpha = 1
if(nargin==2)
    alpha=1;
end
n = length(W);
x = linspace(0,n,n);
if(alpha==Inf)
    H = -log(max(max(W)));
elseif(alpha == 1)
    if(sum(sum(W==0)))==0
        H = -trapz(x,trapz(x,W.*log(W)))*dxdp;
    else
        H = -sum(sum(W(W~=0).*log(W(W~=0))))*dxdp;
    end
else
    int = dxdp*trapz(x,trapz(x,W.^alpha));
    H = (1/(1-alpha))*log(int);
end
end
```

D.3.5 majorizes.m

```
function [bool,min_diff] = majorizes(W,w,tol)
%Returns true if W majorizes w, false otherwise
n2 = length(W)^2;
if(nargin==2)
    tol=10;
end
FdM = fx_dec(W);
Fdm = fx_dec(w);
FdM = FdM/sum(FdM);
Fdm = Fdm/sum(Fdm);
FdMcum = zeros(1,n2);
Fdmcum = zeros(1,n2);
FdMcum(1)=FdM(1);
Fdmcum(1)=Fdm(1);
for i=2:n2
   FdMcum(i) = FdM(i)+FdMcum(i-1);
```

```
    Fdmcum(i) = Fdm(i)+Fdmcum(i-1);
end
bool = true;
diff = FdMcum-Fdmcum;
min_diff = min(diff);
if(min_diff<-(10^(-tol)))
    bool = false;
end
end
```

D.3.6 wig_dec.m

```
function Wd = wig_dec(W,rL)
%Computes the decreasing rearrangement of W
nr = length(W);
dxdp = (rL/nr)^2;
int = linspace(-rL/2,rL/2,nr);
[X,Y]= meshgrid(int);
A = pi*(X.^2+Y.^2);
W = (W+abs(W))/2;
[Fd,Fdint] = fx_dec(W,dxdp);
Wd = interp1(Fdint,Fd,A,'nearest','extrap');
end
```

D.3.7 wig_char.m

```
function Wcar = wig_char(W,rL)
%Computes the characteristic function of W
nr = length(W);
dxdp =(rL/nr)^2;
g = linspace(-rL/2,rL/2,nr);
[U,V] = meshgrid(g);
Wcar = zeros(nr);
E = zeros(nr);
for i=1:nr
    for j=1:nr
        u = U(i,j);
        v = V(i,j);
        E = exp(-2*1i*(u*U+v*V));
        Wcar(i,j) = trapz(g,trapz(g,W.*E));
    end
end
```

D.3.8 wig_fock_ij.m

```
function W = wig_fock_ij(i,j,nr,rL,int)
%Computes W_ij
f_i = fx_fock(i,int);
f_j = fx_fock(j,int);
```

```
[X,P] = meshgrid(int);
W=zeros(nr);
dint = (max(int)-min(int))/(length(int)-1);
for i=1:nr
    for j=1:nr
        x = X(i,j);
        p = P(i,j);
        W(i,j) = (dint/pi) *sum(exp(2*1i*p*int) ...
            .*interp1(int,f_j,x-int,'spline',0) ...
            .*conj(interp1(int,f_i,x+int,'spline',0)));
    end
end
end
```

D.3.9 rad_from_wig.m

```
function [f,int] = rad_from_wig(W,rL)
%Computes the radial function of the decreasing rearrangement of W
nr = length(W);
if nargin == 2
    int = linspace(0,rL,nr);
else
    int = 1:nr;
end
F = reshape(W,1,nr^2);
F = sort(F,'descend');

f = zeros(1,nr);
for i = 1:nr
    ind = round(pi*i^2);
    if ind<nr^2
        f(i) = F(round(pi*i^2));
    end
end
end
```

D.3.10 wig_from_rad.m

```
function W  = wig_from_rad(nr,rL,f,int)
%Computes Wigner function from its radial function
dxdp = (rL/nr)^2;
g = linspace(-rL/2,rL/2,nr);
[X,P] = meshgrid(g);
W = (X.^2+P.^2).^(1/2);
W = interp1(int,f,W,'spline',0);
end
```